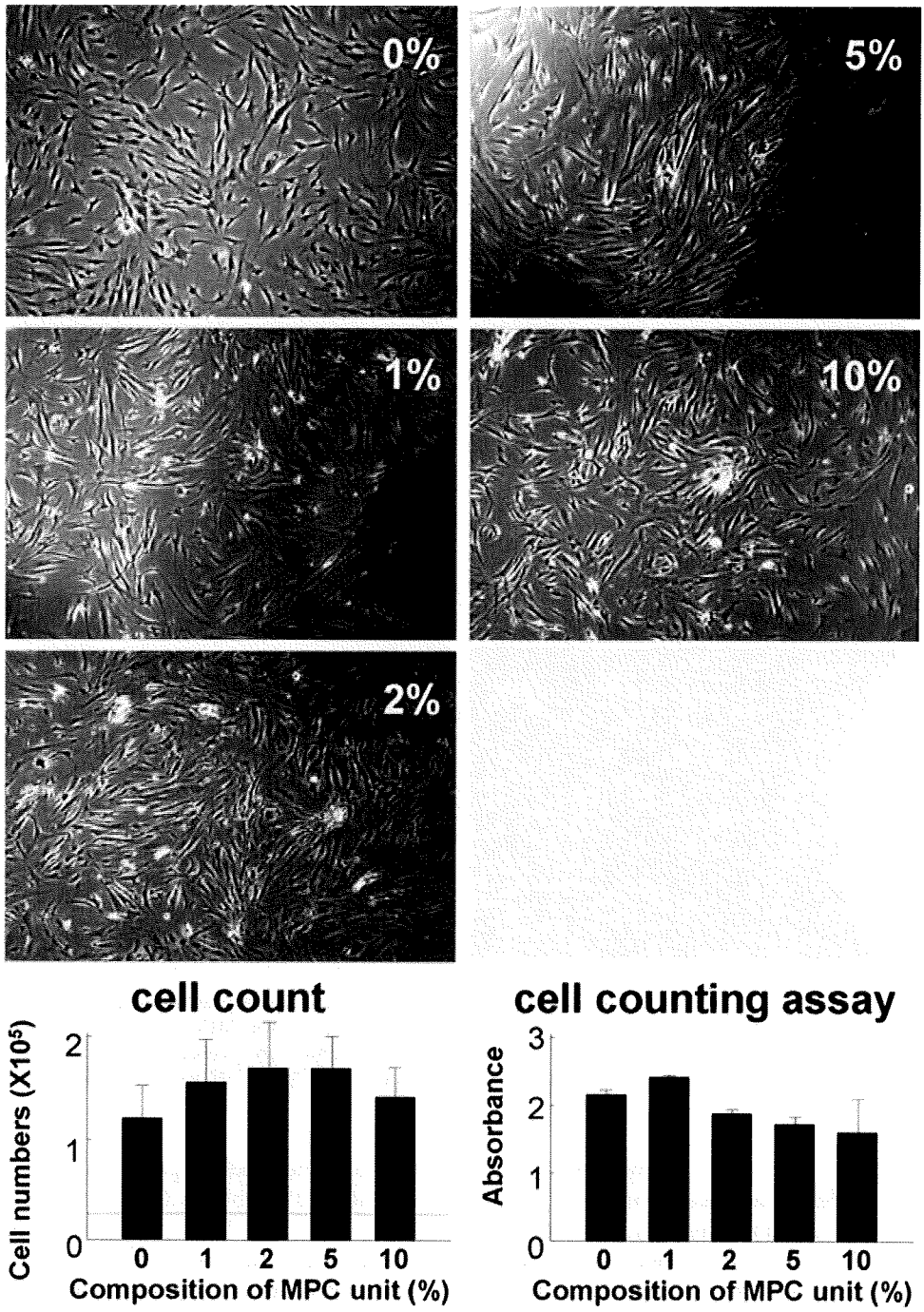

Figure 3. Proliferation of the cells that had been selected by the plate-coated MPC polymer with various MPC unit compositions. The cells cultured on the MPC polymer-coated plates were harvested and then reseeded onto the conventional PS plates. The numbers of human cells were counted at 7 days of culture (cell count). All values are presented as mean plus standard deviation of five samples per group. Statistics were assessed using Dunnett's test. No significant difference was seen among the proliferation of the cells harvested from each MPC polymer-coated plate (0–10% MPC unit composition). The dashed line indicats the number of cells originally seeded on the plate (1.9×10^3 cells). The result was represented by the experiment using the cell counting assay in the rat MSCs (cell counting assay). All values are presented as mean plus standard deviation of three measurements per group. No significant difference (Dunnett's test) was seen among each groups.

luronan receptor), CD105 (Endoglin) and CD166 (ALCAM) were expressed in MSC, but that CD34 and CD45 (LCA) were markers specific for heamatopoietic stem cells. Although the hematopoietic stem cell markers were negative in all cells selected by the plates coated with the 0, 1, 2, 5, or 10% of MPC unit

TABLE I
Expression of Surface Epitopes in MPC-Selected Cells

Surface Epitoptes	MPC 0%	MPC 1%	MPC 2%	MPC 5%	MPC 10%
CD29 (integrin β1)	++	++	+++	++	++
CD44 (Hyaluronan receptor)	++	++	++	++	++
CD105 (Endoglin)	+	+	+	+	+
CD166 (ALCAM)	+	+	+	+	+
CD34	−	−	−	−	−
CD45 (LCA)	−	−	−	−	−

composition, CD29, CD44, CD105, and CD166 were detectable in the cells of all MPC unit compositions. The levels of the MSC markers in the cells selected by the 1–10% MPC unit composition were almost similar to those in cells of 0% that corresponds to the control MSC, implying that the MPC polymer-selected cells belong to the category of MSC on the surface epitopes (Table I).

Osteogenic and chondrogenic potential of MPC polymer-selected cells

After the culture on the MPC polymer-coated plates (passage 1), the cells were cultured on the conventional PS culture plates for a long term with repeated passages. By passage 5, the cell numbers had expanded by approximately 1000-fold in the cells of each MPC unit composition (0–10%). Under the osteogenic condition, the cells selected by the MPC polymer coated-plates and cultured in the conventional PS plate ones for a single time (passage 2) more highly expressed the COL1A1 mRNA in the 2–5% MPC than in the 0%, but those by the 1 or 10% MPC polymer-coated plates did not show any significant increase in the COL1A1 expression. The promotion effects of the COL1A1 expression in 2% MPC unit composition continued even at passage 5, although the cells at passage 2 were more sensitive for the osteogenic differentiation than those at passage 5. ALP also peaks at 2-5% MPC unit composition for both passages, although no statistical difference of the ALP expression was detected in passage 2 [Fig. 4(a)]. The ALP enzyme activity was also significantly higher in 5% MPC unit composition than others at passage 2 [Fig. 4(b)].

The expression of the chondrocyte markers in the MPC polymer-selected cells under the chondrogenic conditions was also enhanced in the 2–5% MPC unit composition, as observed during osteogenesis. Responding to the chondrogenic induction, the cells began to express COL2A1, COL10A1, and Sox 9, and especially cells selected by the 2% MPC unit composition showed a prominent expression of all chondrocyte markers not only at passage 2, but even at passage 5 (Fig. 5).

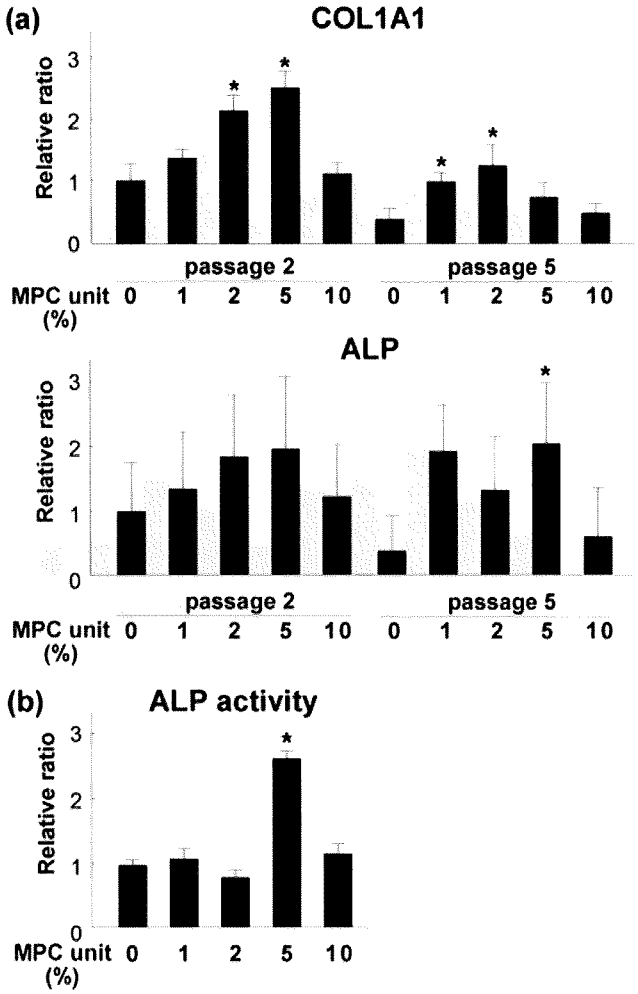

Figure 4. (a) Gene expression of COL1A1 and ALP in the osteogenic induction. Significant expression of COL1A1 gene was found in human MSCs selected by the MPC polymer-coated plates (2–5% unit composition) at passage 2, while the high expression level in the 5% MPC unit composition continued by passage 5. Also, in the ALP expression, the promotion effect was observed in 2–5% MPC unit composition, especially at passage 5. All values are presented as mean plus standard deviation of five samples per group. Statistics were assessed using Dunnett's test (*$p < 0.01$ vs. 0% MPC unit composition). (b) The enzyme activity for ALP in the osteogenic induction. The ALP enzyme activity was also significantly higher in 5% MPC unit composition than others in the rat MSCs at passage 2. All values are presented as mean plus standard deviation of three measurements per group. Statistics were assessed using Dunnett's test (*$p < 0.01$ vs. 0% MPC unit composition).

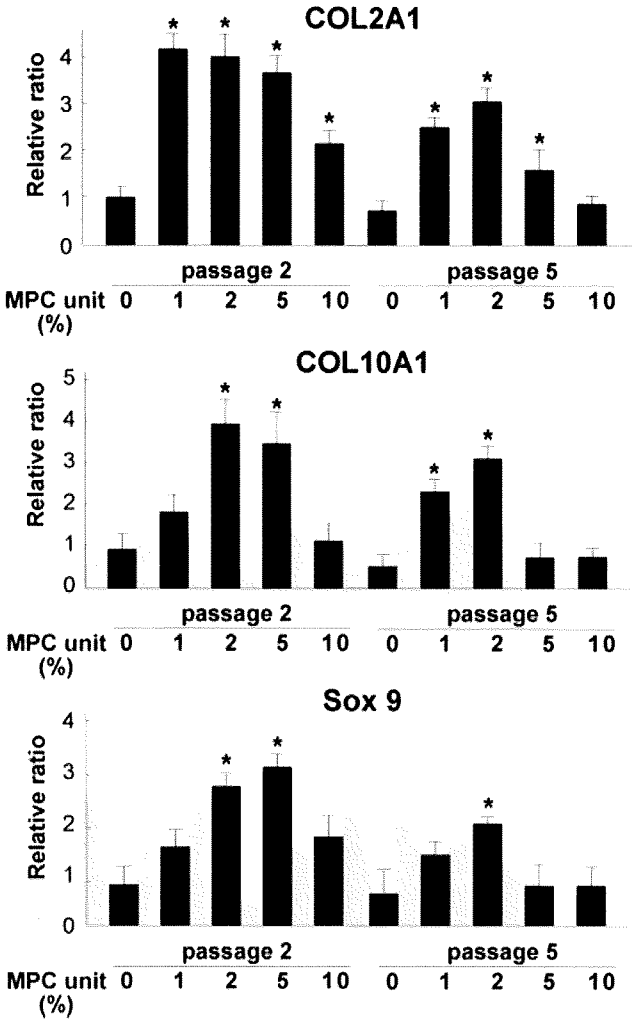

Figure 5. Gene expression of COL2A, COL10A1, and Sox9 during the chondrogenic induction. The expressions of COL2A1, COL10A1, and Sox9 genes peaked at 2–5% MPC unit composition not only at passage 2 but also at passage 5. All values are presented as mean plus standard deviation of five samples per group. Statistics were assessed using Dunnett's test (*$p < 0.01$ vs. 0% MPC unit composition).

DISCUSSION

The adhesion capacity seems to have some association with the cellular activities and functions. Specific adhesion to the laminin and type IV collagen coated on the surface of the culture dishes could select the myogenic cells of the embryonic mouse thigh from fibroblastic cells. Over a brief time period (10–20 min), myoblasts from the embryonic mouse thigh muscle had adhered faster to the laminin than did the fibroblasts from the same tissue, while the latter adhered faster to the fibronectin than the former.[19] Laminin-1 also enriched the osteoblast progenitor cells from rat calvarial cells when they were seeded on the culture wells coated with it. The laminin-1 inhibited cell attachment of the rat calvarial cells, but could select the highly osteogenic lineage according to the difference in the cell adhesiveness to that of the molecule.[20] Thus, through the selection of the cell adhesion to some molecules, a specific cell subpopulation that possesses a high differentiation potency would be concentrated from heterogeneity of the cell sources.

MSC expresses many adhesion-related molecules, like the integrin subunits α4, 5, 6, 8, 9, v/β1, 3, 5, ICAM-1, ALCAM, VCAM-1, SCF, fibronection, E-cadherin, and hyaluronan receptor[21–23] and can be bound to various ligands including laminin and E-cadherin to play biological roles through the cell-to-cell or cell-to-matrix contacts. As examples of the cell-to-cell contact with MSCs *in vivo*, homing functions for the hematopoietic cells of MSCs should be discussed. Through the cell-to-cell contacts with hematopoietic stem cells mediated by VCAM-1, fibronectin, SCF, E-cadherin, or ICAM-1, MSCs secrete extracellular matrix proteins, produce secreted/membrane-bound cytokines and regulate hematopoiesis.[22] MSCs are also recruited and adhered to the damaged tissues in order to participate in tissue repair. These cells can provide cell sources for tissue repair in bone, cartilage, and even skeletal muscle or myocardium that do not directly make contact with bone marrow. Once muscles are injured, the MSCs are delivered to the degenerative muscles from the circulation, are adhered to the lesion, take part in the regenerative process, and provide fully differentiated muscle fibers.[24] In the murine model of cardiac repair following ischemic injury, MSCs were mobilized from bone marrow, homed and generated cardiac myocytes. Among the adhesion molecules of the MSC such as integrin α4, 6, 8, 9, and β1, blockade of the integrin β1 by the neutralizing antibody reduced the total number of MSCs in the infracted myocardium, suggesting that MSCs utilized integrin β1 for cell adhesion to the myocardium and its regeneration.[23]

Thus, MSCs can be bound to various partners via many kinds of adhesion molecules to exert physiological and pathological functions. Although the adhesiveness to some ligands likely selects a cell subpopulation with a high differentiation potency of a certain lineage,[19,20] such a specific selection may have the risk to reduce the multipotency in MSCs. Therefore, we applied the selection system based not on the adhesiveness to specific molecules, but on the general adhesion ability to the MPC polymer-coated plates. As a result, we could enrich the cells to have a high potency of both osteogenesis and chondrogenesis from the crude MSCs.

It has yet remained unknown why the strength of the adhesion ability in MSCs could enhance not the proliferation rate of the cells, but the differential

potential for both osteogenesis and chondrogenesis. Speculating that such multipotent cells may show a stronger adhesion than fibroblastic cells in bone marrow, the MPC polymer-selection due to cell attachment could exclude the fibroblastic ones that possess a lower differentiation potential. This selection probably enriched the cells with high differentiation potential. It implied not that the MPC polymer-coated plates did not induce the phenotype changes in each cell, but that they purified the cell populations by the elimination of fibroblastic cells from the total populations of bone marrow adhesive cells. Therefore, the difference in osteogenic and chondrogenic ability was maintained during the repeated passaging, and the MPC polymer selection could improve cellular potential even after recultivation on PS plates. However, as we do not currently possess the methods to exactly distinguish MSCs from fibroblastic cells using cell surface epitopes, it may be hard to prove that the MPC selection could concentrate the multipotent MSCs from a mixture of the MSCs with fibroblast, by flow cytometry that can exactly exclude the hematopoietic lineage from the MSCs.

MSC can be differentiated into a variety of tissues including bone, cartilage, tendon, fat, heart, muscle or brain, *in vitro* and *in vivo*.[1,8] Autologous MSCs have advantages over embryonic stem cells, regarding the teratocarcinoma formation, immune rejection, or ethical problems. The cell sources have already been used for the treatment of osteogenesis imperfecta, bone/cartilage defects, myocardiac infarction, or skin ulcer.[25–28] Conversely, the MPC polymers have also been already applied in the clinical field for the surfaces of intravascular stents, intravascular guide wires, soft contact lenses, and the artificial lung, all of which were authorized by the United States Food and Drug Administration.[13,14] Thus, the biocompatible polymer is regarded to be approved for safe clinical use.

The MPC selection is as simple as to culture MSCs with MPC polymer-coated plates in the first passage, which would reduce the risks of contamination or mismanagement during the culture procedure. The improvement of the MSCs in purity and multipotency by the MPC polymer selection would provide promising technologies for the next generation-cell therapy that can be applied for more severe and other various diseases. The clinical application of the MPC polymer-selected MSCs is now underway.

References

1. Pittenger MF, Mackay AM, Beck SC, Jaiswal RK, Douglas R, Mosca JD, Moorman MA, Simonetti DW, Craig S, Marshak DR. Multilineage potential of adult human mesenchymal stem cells. Science 1999;284:143–147.
2. Makino S, Fukuda K, Miyoshi S, Konishi F, Kodama H, Pan J, Sano M, Takahashi T, Hori S, Abe H, Hata J, Umezawa A, Ogawa S. Cardiomyocytes can be generated from marrow stromal cells in vitro. J Clin Invest 1999;103:697–705.
3. Kopen GC, Prockop DJ, Phinney DG. Marrow stromal cells migrate throughout forebrain and cerebellum, and they differentiate into astrocytes after injection into neonatal mouse brains. Proc Natl Acad Sci USA 1999;96:10711–10716.
4. Friedenstein AJ, Deriglasova UF, Kulagina NN, Panasuk AF, Rudakowa SF, Luria EA, Ruadkow IA. Precursors for fibroblasts in different populations of hematopoietic cells as detected by the in vitro colony assay method. Exp Hematol 1974;2:83–92.
5. Sekiya I, Larson BL, Vuoristo JT, Cui JG, Prockop DJ. Adipogenic differentiation of human adult stem cells from bone marrow stroma (MSCs). J Bone Miner Res 2004;19:256–264.
6. Colter DC, Sekiya I, Prockop DJ. Identification of a subpopulation of rapidly self-renewing and multipotential adult stem cells in colonies of human marrow stromal cells. Proc Natl Acad Sci USA 2001;98:7841–7845.
7. Smith JR, Pochampally R, Perry A, Hsu SC, Prockop DJ. Isolation of a highly clonogenic and multipotential subfraction of adult stem cells from bone marrow stroma. Stem Cells 2004;22:823–831.
8. Ishii M, Koike C, Igarashi A, Yamanaka K, Pan H, Higashi Y, Kawaguchi H, Sugiyama M, Kamata N, Iwata T, Matsubara T, Nakamura K, Kurihara H, Tsuji K, Kato Y. Molecular markers distinguish bone marrow mesenchymal stem cells from fibroblasts. Biochem Biophys Res Commun 2005;332: 297–303.
9. Pochampally RR, Smith JR, Ylostalo J, Prockop DJ. Serum deprivation of human marrow stromal cells (hMSCs) selects for a subpopulation of early progenitor cells with enhanced expression of OCT-4 and other embryonic genes. Blood 2004; 103:1647–1652.
10. Ueda H, Watanabe J, Konno T, Takai M, Saito A, Ishihara K. Asymmetrically functional surface properties on biocompatible phospholipid polymer membrane for bioartificial kidney. J Biomed Mater Res A 2006;77:19–27.
11. Sawada S, Iwasaki Y, Nakabayashi N, Ishihara K. Stress response of adherent cells on a polymer blend surface composed of a segmented polyurethane and MPC copolymers. J Biomed Mater Res A 2006;79:476–484.
12. Sibarani J, Takai M, Ishihara K. Surface modification on microfluidic devices with 2-methacryloyloxyethyl phosphorylcholine polymers for reducing unfavorable protein adsorption. Colloids Surf B Biointerfaces 2007;54:88–93.
13. Lewis AL, Tolhurst LA, Stratford PW. Analysis of a phosphorylcholine-based polymer coating on a coronary stent pre- and post-implantation. Biomaterials 2002;23:1697–1706.
14. Kihara S, Yamazaki K, Litwak KN, Litwak P, Kameneva MV, Ushiyama H, Tokuno T, Borzelleca DC, Umezu M, Tomioka J, Tagusari O, Akimoto T, Koyanagi H, Kurosawa H, Kormos RL, Griffith BP. In vivo evaluation of a MPC polymer coated continuous flow left ventricular assist system. Artif Organs 2003;27:188–192.
15. Moro T, Takatori Y, Ishihara K, Konno T, Takigawa Y, Matsushita T, Chung UI, Nakamura K, Kawaguchi H. Surface grafting of artificial joints with a biocompatible polymer for preventing periprosthetic osteolysis. Nat Mater 2004;3:829–836.
16. Goda T, Ishihara K. Soft contact lens biomaterials from bioinspired phospholipid polymers. Expert Rev Med Devices 2006;3:167–174.
17. Kato Y, Iwamoto M, Koike T, Suzuki F, Takano Y. Terminal differentiation and calcification in rabbit chondrocyte cultures grown in centrifuge tubes: Regulation by transforming growth factor beta and serum factors. Proc Natl Acad Sci USA 1988;85:9552–9556.

18. Ebisawa K, Hata K, Okada K, Kimata K, Ueda M, Torii S, Watanabe H. Ultrasound enhances transforming growth factor β-mediated chondrocyte differentiation of human mesenchymal stem cells. Tissue Eng 2004;10:921–929.
19. Kuhl U, Ocalan M, Timpl R, von der Mark K. Role of laminin and fibronectin in selecting myogenic versus fibrogenic cells from skeletal muscle cells in vitro. Dev Biol 1986;117:628–635.
20. Roche P, Rousselle P, Lissitzky JC, Delmas PD, Malaval L. Isoform-specific attachment of osteoprogenitors to laminins: Mapping to the short arms of laminin-1. Exp Cell Res 1999;250:465–474.
21. Conget PA, Minguell JJ. Phenotypical and functional properties of human bone marrow mesenchymal progenitor cells. J Cell Physiol 1999;181:67–73.
22. Hall BM, Gibson LF. Regulation of lymphoid and myeloid leukemic cell survival: Role of stromal cell adhesion molecules. Leuk Lymphoma 2004;45:35–48.
23. Ip JE, Wu Y, Huang J, Zhang L, Pratt RE, Dzau VJ. Mesenchymal stem cells utilize integrin beta 1 not CXC chemokine receptor 4 for myocardial migration and engraftment. Mol Biol Cell 2007;18:2873–2882.
24. Ferrari G, Cusella-De Angelis G, Coletta M, Paolucci E, Stornaiuolo A, Cossu G, Mavilio F. Muscle regeneration by bone marrow-derived myogenic progenitors. Science 1998;279:1528–1530.
25. Horwitz EM, Prockop DJ, Fitzpatrick LA, Koo WW, Gordon PL, Neel M, Sussman M, Orchard P, Marx JC, Pyeritz RE, Brenner MK. Transplantability and therapeutic effects of bone marrow-derived mesenchymal cells in children with osteogenesis imperfecta. Nat Med 1999;5:309–313.
26. Quarto R, Mastrogiacomo M, Cancedda R, Kutepov SM, Mukhachev V, Lavroukov A, Kon E, Marcacci M. Repair of large bone defects with the use of autologous bone marrow stromal cells. N Engl J Med 2001;344:385–386.
27. Vojtassak J, Danisovic L, Kubes M, Bakos D, Jarabek L, Ulicna M, Blasko M. Autologous biograft and mesenchymal stem cells in treatment of the diabetic foot. Neuro Endocrinol Lett 2006;27(Suppl 2):134–1371.
28. Fox JM, Chamberlain G, Ashton BA, Middleton J. Recent advances into the understanding of mesenchymal stem cell trafficking. Br J Haematol 2007;137:491–502.

Biomaterials 31 (2010) 658–668

Contents lists available at ScienceDirect

Biomaterials

journal homepage: www.elsevier.com/locate/biomaterials

Lubricity and stability of poly(2-methacryloyloxyethyl phosphorylcholine) polymer layer on Co–Cr–Mo surface for hemi-arthroplasty to prevent degeneration of articular cartilage

Masayuki Kyomoto [a,c,f], Toru Moro [c,d], Ken-ichi Saiga [a,c,f], Fumiaki Miyaji [f], Hiroshi Kawaguchi [d], Yoshio Takatori [c,d], Kozo Nakamura [d], Kazuhiko Ishihara [a,b,e,*]

[a] Department of Materials Engineering, The University of Tokyo, 7-3-1 Hongo, Bunkyo-ku, Tokyo 113-8654, Japan
[b] Department of Bioengineering, School of Engineering, The University of Tokyo, 7-3-1 Hongo, Bunkyo-ku, Tokyo 113-8654, Japan
[c] Division of Science for Joint Reconstruction, Graduate School of Medicine, The University of Tokyo, 7-3-1 Hongo, Bunkyo-ku, Tokyo 113-8654, Japan
[d] Sensory & Motor System Medicine, Faculty of Medicine, The University of Tokyo, 7-3-1 Hongo, Bunkyo-ku, Tokyo 113-8654, Japan
[e] Center for NanoBio Integration, The University of Tokyo, 7-3-1 Hongo, Bunkyo-ku, Tokyo 113-8654, Japan
[f] Research Department, Japan Medical Materials Corporation, 3-3-31 Miyahara, Yodogawa-ku, Osaka 532-0003, Japan

ARTICLE INFO

Article history:
Received 30 July 2009
Accepted 22 September 2009
Available online 9 October 2009

Keywords:
Phosphorylcholine
Cobalt alloy
Hip replacement prosthesis
Surface modificaiton
Cartilage
Friction

ABSTRACT

Migration of the artificial femoral head to the inside of the pelvis due to the degeneration of acetabular cartilage has emerged as a serious issue in resurfacing or bipolar hemi-arthroplasty. Surface modification of cobalt–chromium–molybdenum alloy (Co–Cr–Mo) is one of the promising means of improving lubrication for preventing the migration of the artificial femoral head. In this study, we systematically investigated the surface properties, such as lubricity, biocompatibility, and stability of the various modification layers formed on the Co–Cr–Mo with the biocompatible 2-methacryloyloxyethyl phosphorylcholine (MPC) polymer by dip coating or grafting. The cartilage/poly(MPC) (PMPC)-grafted Co–Cr–Mo interface, which mimicked a natural joint, showed an extremely low friction coefficient of <0.01, as low as that of a natural cartilage interface. Moreover, the long-term stability in water was confirmed for the PMPC-grafted layer; no hydrolysis of the siloxane bond was observed throughout soaking in phosphate-buffered saline for 12 weeks. The PMPC-grafted Co–Cr–Mo femoral head for hemi-arthroplasty is a promising option for preserving acetabular cartilage and extending the duration before total hip arthroplasty.

1. Introduction

Resurfacing or bipolar hemi-arthroplasty for the treatments of osteoarthritis or osteonecrosis of hip of the young, active patient profile, and fractures of the femur neck of the typically aged patient profile, has long been advocated [1]. Consequently, resurfacing and bipolar hemi-arthroplasties can be possibly used as delaying tactics prior to revision surgeries of total hip arthroplasty. Most patients receive dramatic pain relief and rapid improvement in both their daily activities and quality of life due to advantages such as reduced blood loss, lower dislocation, ease of implantation, etc. However, migration of the artificial femoral head to the inside of the pelvis due to the degeneration of acetabular cartilage has emerged as a serious issue in the hemi-arthroplasties [2]. The longevity of the artificial femoral head after hemi-arthroplasty depends upon the quality of the acetabular cartilage or the lubrication conditions between the artificial femoral head and acetabular cartilage. Surface modifications of cobalt–chromium–molybdenum alloy (Co–Cr–Mo) for the artificial femoral head is one of the promising means of improving lubrication and preventing the degradation of acetabular cartilage, thereby preventing the migration of the artificial femoral head. Such surface modifications may improve hemi-arthroplasty survival, and liberate the restrictions for its application to younger, active patients.

Most frequently, surface modification with polymer is performed using either of the following methods: (1) surface-initiated graft polymerization, termed as the "grafting from" method, in which monomers are polymerized from initiators, and the polymeric molecules are grafted onto the substrate through covalent bonding; and (2) adsorption or immobilization of the polymer onto

* Corresponding author. Department of Materials Engineering, School of Engineering, The University of Tokyo, Hongo 7-3-1, Bunkyo-ku, Tokyo 113-8656, Japan. Tel.: +81 3 5841 7124; fax: +81 3 5841 8647.
E-mail address: ishihara@mpc.t.u-tokyo.ac.jp (K. Ishihara).

0142-9612/$ – see front matter © 2009 Elsevier Ltd. All rights reserved.
doi:10.1016/j.biomaterials.2009.09.083

the substrate (i.e., dipping, cross-linking, and ready-made polymers with reactive end groups reacting with the functional groups of the substrate) [3–5].

2-Methacryloyloxyethyl phosphorylcholine (MPC) polymers have attracted considerable attention as surface modifiable polymers for several medical devices [6–16]. MPC is a monomer for preparing novel polymer biomaterials and can undergo conventional radical copolymerization with other methacrylates, such as *n*-butyl methacrylate (BMA), *n*-dodecyl methacrylate (DMA), and 3-methacryloxypropyl trimethoxysilane (MPSi), to form poly (MPC-*co*-BMA), poly(MPC-*co*-DMA), and poly(MPC-*co*-MPSi), respectively [10–16]. They have potential applications in a variety of fields such as biomedical science, surface science, and bioengineering because they possess unique properties such as excellent anti-biofouling ability and low friction ability. Thus, surface modification with the MPC polymer on medical devices is effective for obtaining biocompatibility. In fact, several medical devices have already been developed by utilizing MPC polymers and used clinically; therefore, the efficacy and safety of MPC polymers as biomaterials are well established [14–16].

In this study, we hypothesize that the structure of surface modification layers might affect the long-term stability, hydration kinetics, articular cartilage retention, etc., and particularly that the poly(MPC) (PMPC)-grafted surface might assure the long-term performance of the artificial femoral head for partial hemiarthroplasty. Therefore, we investigated the surface properties of various surface modification layers with the MPC polymer and the effects of the surface properties on the friction of the artificial femoral head against articular cartilage. The results reveal that the structure of the PMPC-grafted layer on the Co–Cr–Mo surface plays an important role in the articular cartilage retention in the long term.

2. Materials and methods

2.1. Chemicals

MPC was industrially synthesized by using the method reported by Ishihara et al. and supplied by NOF Corp. (Tokyo, Japan) [17]. MPSi was purchased from Shin-Etsu Chemical Co., Ltd. (Tokyo, Japan). Succinic acid and ethanol were purchased from Kanto Chemical Co., Inc. (Tokyo, Japan). 2-Hydroxy-l-[4-(hydroxyethoxy) phenyl]-2-methyl-propan-1-one (DAROCUR 2959; D2959), as a highly efficient radical photoinitiator for ultraviolet (UV) curing, was purchased from Ciba Specialty Chemicals Holding Inc. (Basel, Switzerland) Poly(MPC-*co*-BMA) (PMB30; MPC unit mole fraction = 0.3) [17], poly(MPC-*co*-MPSi) (PMSi90; MPC unit mole fraction = 0.9) [13], and PMPC (for lubricant additive in friction test) were synthesized in ethanol using 2,2′-azobisisobutyronitrile as an initiator by a conventional radical copolymerization method.

2.2. Co–Cr–Mo alloy substrate and pretreatments

The Co–Cr–Mo alloy was supplied by Yoneda Advanced Casting Co., Ltd (Takaoka, Japan). This alloy was manufactured according to the ASTM F75 standard specification for the Co–28Cr–6Mo alloy. The Co–Cr–Mo samples were machined and polished so that the average surface roughness was approximately 0.01 μm; this surface was comparable to those of femoral ball products.

The polished Co–Cr–Mo samples were washed with acetone, and then immersed in 35 vol% nitric acid at room temperature for 35 min. This treatment aimed at passivation by surface oxidation; this would lead to the dissolution of certain foreign substance residues and the concentration of the Cr constituent by "resurfacing" [18]. After the nitric acid treatment, the Co–Cr–Mo samples were irradiated with O_2 plasma at a 500-W high-frequency output and 150-mL/min O_2 gas flow for 5 min by using an O_2 plasma etcher (PR500; Yamato Scientific Co., Ltd., Tokyo, Japan). The O_2 plasma treatment increased the thickness of the surface oxide layer [18].

2.3. MPC polymer coating

The preparation of the MPC polymer-coated Co–Cr–Mo is schematically illustrated in Fig. 1. The physical adsorption of PMB30 was carried out by the solvent evaporation method, where the pretreated Co–Cr–Mo specimens were dipped into ethanol solution containing 0.2 mass% PMB30 ($Mw = 6.0 \times 10^5$) for 10 s for coating and then placed in an ethanol vapor atmosphere at room temperature for 1 h. The coated Co–Cr–Mo specimens were again dipped for 10 s and placed in the ethanol vapor atmosphere at room temperature for 1 h (PMB30-adsorbed Co–Cr–Mo).

The chemical immobilization of PMSi90 was also carried out by the solvent evaporation method. The pretreated Co–Cr–Mo specimens were dipped into ethanol solution containing 0.5 mass% PMSi90 ($Mw = 9.8 \times 10^4$) and 0.063 mg/mL succinic acid for 12 h for the silanization of trimethoxysilane group of PMSi90 and placed in the ethanol vapor atmosphere at room temperature for 1 h. The coated Co–Cr–Mo specimens were annealed in air at 70 °C for 3 h for dehydration (PMSi90-immobilized Co–Cr–Mo).

2.4. MPSi silanization and MPC graft polymerization

The preparation of the PMPC-grafted Co–Cr–Mo is schematically shown in Fig. 1. The pretreated Co–Cr–Mo samples were immersed in an ethanol solution containing 5 mass% MPSi, 1 mass% succinic acid, and 0.1 mass% D2959 at room temperature for 12 h for silanization of the trimethoxysilane group. In this study, D2959 was used as a photoinitiator for surface-initiated polymerization so as to be included in the MPSi layer. They were then annealed at 70 °C for 3 h in air for dehydration. MPC was dissolved in degassed pure water to obtain a concentration of 0.5 mol/L. Subsequently, the MPSi (containing D2959)-coated Co–Cr–Mo samples were immersed in MPC aqueous solutions. Photoinduced graft polymerization on the Co–Cr–Mo surface was performed using ultraviolet irradiation (UVL-400HA ultra-high pressure mercury lamp; Riko-Kagaku Sangyo Co., Ltd., Funabashi, Japan) with an intensity of 5 mW/cm^2 at 60 °C for 90 min; a filter (Model D-35; Toshiba Co., Tokyo, Japan) was used to restrict the passage of ultraviolet light to wavelengths of 350 ± 50 nm (PMPC-grafted Co–Cr–Mo) [19]. After the polymerization, the PMPC-grafted Co–Cr–Mo samples were removed from the solution, washed with pure water and ethanol, and dried at room temperature. The molecular weight of the PMPC graft chain on the PMPC-grafted Co–Cr–Mo samples could not be determined due to the difficulty in separating the PMPC graft chain from the Co–Cr–Mo substrate. Additional efforts are needed in this aspect.

2.5. Articular cartilage from porcine ankle joint

Articular cartilage specimens were harvested from the flat part of the ankle joint of the fresh frozen porcine tibia (age 6–9 months) by using a surgical saw for the friction test. The pin-type (cylinder-shaped with a height of 5 mm and diameter of 9 mm) articular cartilage specimens had approximately a 1-mm cartilage layer and the subcondral bone used for mounting. Throughout the procedure, the articular cartilage surface was hydrated regularly with Dulbecco's phosphate-buffered saline (PBS, pH 7.4, ion strength = 0.15 M; Immuno-Biological Laboratories Co., Ltd., Takasaki, Japan).

2.6. Surface analysis of surface-modified Co–Cr–Mo with various MPC polymers

The functional group vibrations of the surface-modified Co–Cr–Mo samples were examined by Fourier-transform infrared (FT-IR) spectroscopy with attenuated total reflection (ATR) equipment. The FT-IR/ATR spectra were obtained using an FT-IR analyzer (FT/IR615; JASCO Co. Ltd., Tokyo, Japan) for 32 scans over the range from 800 to 2000 cm^{-1} at a resolution of 4.0 cm^{-1}.

The surface elemental conditions of the surface-modified Co–Cr–Mo samples were analyzed by X-ray photoelectron spectroscopy (XPS). The XPS spectra were obtained using an XPS spectrophotometer (AXIS-HSi165, Kratos/Shimadzu Co., Kyoto, Japan) equipped with a 15-kV Mg-Kα radiation source at the anode. The take-off angle of the photoelectrons was maintained at 90°. Five scans were taken for each sample.

The static-water contact angles on the surface-modified Co–Cr–Mo samples were measured by the sessile drop method using an optical bench-type contact angle goniometer (Model DM300, Kyowa Interface Science Co., Ltd., Saitama, Japan). Drops of purified water (1 μL) were deposited on the surface-modified Co–Cr–Mo surfaces, and the contact angles were directly measured with a microscope after 60 s of dropping. Measurements were repeated fifteen times for each sample, and the average values were regarded as the contact angles.

The surface-modified Co–Cr–Mo samples were stained with rhodamine 6G (Wako Pure Chemical Industries, Ltd., Osaka, Japan) and observed by fluorescence microscopy (FM). According to previous literature, rhodamine 6G effectively stains the MPC polymer, which possesses great structural similarity to lipids [20]. This simple staining technique enables the evaluation of the surface-modified layer with MPC polymer by FM. An aqueous solution of 200 mass ppm rhodamine 6G was used for all the staining experiments. The samples were immersed in the rhodamine 6G solution for 30 s and then removed. Then, they were washed two times consecutively in distilled water for 30 s and then dried. A fluorescence microscope (Axioskop 2 Plus, Carl Zeiss AG, Oberkochen, Germany) was used for FM imaging and examination of all samples. Pseudo-color images were obtained using a charge coupled device (CCD) camera (VB-7010, Keyence Co., Osaka, Japan) and imaging software (VH analyzer 2.51). Lenses with ×10 magnification and appropriate exposure time (approximately 0.1 s) were employed to obtain the best image quality of the various samples.

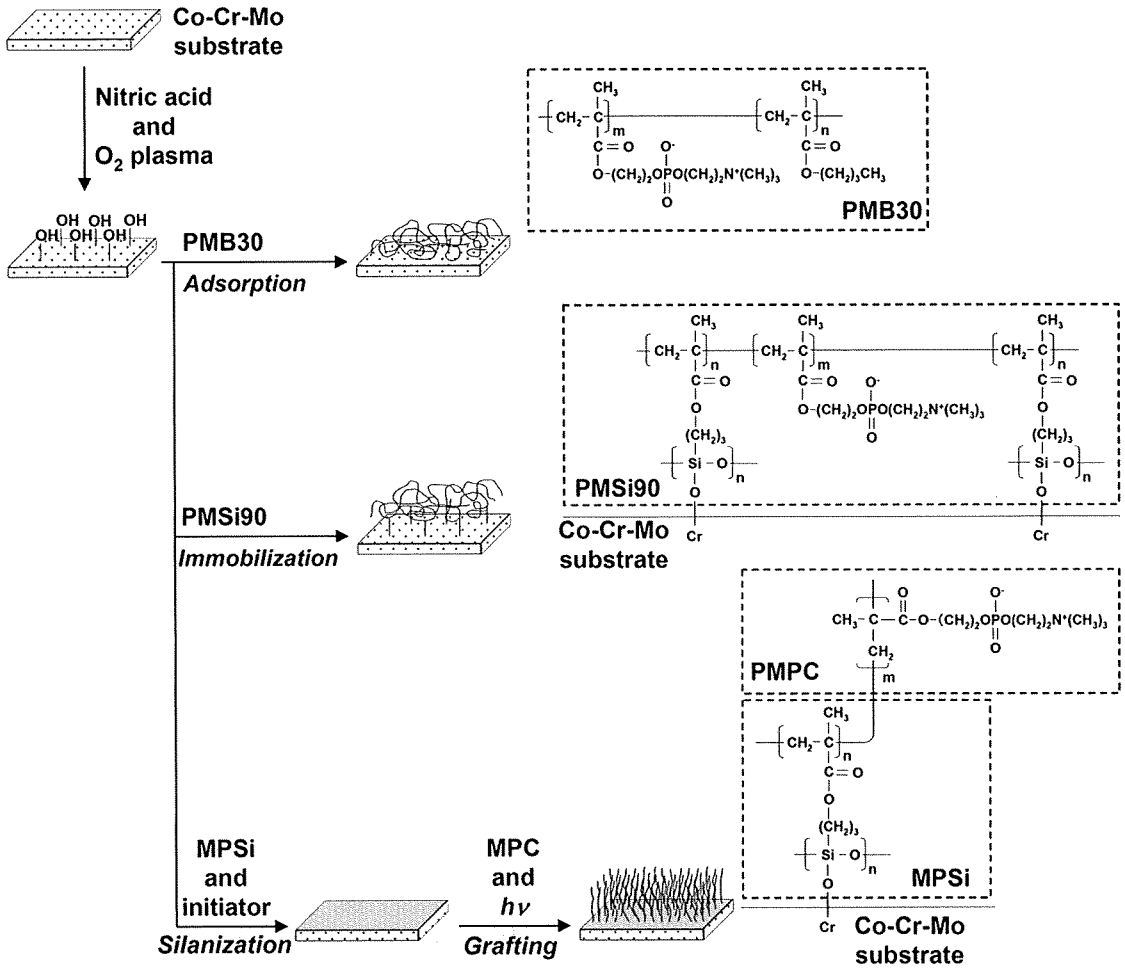

Fig. 1. Schematic illustration for the preparation of MPC polymer-coated and PMPC-grafted Co–Cr–Mo.

2.7. Cross-sectional observation by transmission electron microscopy

A cross-section of the surface-modified Co–Cr–Mo samples was observed using a transmission electron microscope (TEM) and by energy dispersive X-ray (EDX) spectroscopy. The specimens were precoated with an aluminum film; then, a thin film of the samples was prepared by the focused ion beam (FIB) technique using an FB-2000A (Hitachi High-Technologies Co., Tokyo, Japan) FIB system. The samples were thinned to electron transparency by a low gallium ion beam current. The thin film thus prepared was positioned onto a copper TEM mesh grid. TEM observations were then recorded using an HF-2000 electron microscope (Hitachi High-Technologies Co.) at an acceleration voltage of 200 kV. EDX spectra were analyzed on a cross-section of the samples using a Sigma EDX attachment (Kevex Instruments, Inc., Valencia, CA, USA) at an acceleration voltage of 200 kV.

2.8. Characterization of protein adsorption by micro bicinchoninic acid method

The amounts of protein adsorbed on the surface-modified Co–Cr–Mo samples were determined by the micro bicinchoninic acid (BCA) method. Each specimen was immersed in PBS for 1 h to equilibrate the surface modified by the MPC polymer. The specimens were immersed in bovine serum albumin (BSA, Mw = 6.7×10^4; Sigma–Aldrich Corp., MO, USA), bovine blood γ-globulins (Mw = 1.5×10^5; Sigma–Aldrich Co.), and bovine plasma fibrinogen (Mw = 3.4×10^5; Sigma–Aldrich Co.) solutions at 37 °C for 1 h. The protein solutions were prepared in BSA, γ-globulins, and fibrinogen concentrations of 4.5, 1.6, and 0.3 g/L, respectively, i.e., 10% of the concentration of human plasma levels. Then, the specimens were rinsed five times with fresh PBS and immersed in 1 mass% sodium dodecyl sulfate (SDS) aqueous solution and shaken at room temperature for 1 h to completely detach the adsorbed BSA, γ-globulins, and fibrinogen on the surface modified by the MPC polymer. A protein analysis kit (micro BCA protein assay kit, #23235; Thermo Fisher Scientific Inc., IL, USA) based on the BCA method was used to determine the BSA concentration in the SDS solution, and the amount of BSA, γ-globulins, and fibrinogen adsorbed on the surface modified by the MPC polymer was calculated.

2.9. Friction test and histological observation of articular cartilage

The coefficients of dynamic friction between the pins fabricated from articular cartilage and the surface-modified Co–Cr–Mo plates were measured by using a pin-on-plate machine (Tribostation 32; Shinto Scientific Co., Ltd., Tokyo, Japan). The friction tests were performed at room temperature and 37 °C with various loads in the range from 0.49 to 9.80 N, sliding distance of 25 mm, and frequency of 1 Hz for a maximum of 5×10^3 cycles [21]. Pure water, mixture of 25 vol% bovine serum (BS), 20 mM/L of ethylene diamine tetraacetic acid (EDTA), 0.1 mass% sodium azide, and the BS mixture containing 0.02 mass% MPC polymer (PMB30 (Mw = 5.0×10^4), PMSi90 (Mw = 9.8×10^4), and PMPC (Mw = 1.0×10^5)) were used as a lubricant each. Subsequently, five replicate measurements were performed for each sample, and the average values were regarded as the coefficients of dynamic friction. After 100 cycles of friction tests, the plate samples were FM-observed. Then, after 5×10^3 cycles friction test, articular cartilage pins against the untreated Co–Cr–Mo and PMPC-grafted Co–Cr–Mo were fixed with 10% neutral buffered formalin for 3 d, then decalcified in KC-X solution (Falma Co., Tokyo, Japan) for 8 d, and then dehydrated in graded ethanol for histological observation. The decalcified cartilage specimens were embedded in paraffin (Tissue-prep; Fisher Scientific Corp., Fair Lawn, NJ, USA), and microsections were prepared and stained with hematoxylin (Real hematoxylin; Dako Co., Carpinteria, CA, USA) and eosin (Eosin yellowish; Kanto Chemical Co., Inc.) (H&E) as well as with Safranin O (Nacalai Tesque, Inc., Kyoto, Japan) and observed with a microscope (Eclipse E600; Nikon Corp., Tokyo, Japan) equipped with a CCD camera (DP72; Olympus Co., Tokyo, Japan).

2.10. PBS soaking test

The surface-modified Co–Cr–Mo samples ($10 \times 10 \times 1$ mm^3 in size) were soaked in 50 mL of PBS. After soaking with 120 rpm shaking at 37 °C for 1, 4, 8, and 12 weeks, the samples removed from the PBS and were characterized by XPS analysis, water-contact angle measurement, and FM observation.

Table 1
Surface elemental composition ($n = 5$) and static-water contact angle ($n = 15$) of untreated, MPC polymer-coated and PMPC-grafted Co–Cr–Mo alloy.

Sample	Surface elemental composition (atom%)								Contact angle (deg)
	C_{1s}	O_{1s}	N_{1s}	P_{2p}	Si_{2p}	Co_{2p}	Cr_{2p}	Mo_{3d}	
Co–Cr–Mo (untreated)	14.6	52.9	0.0	0.0	0.0	26.7	5.4	0.4	81.6
	(1.3)[a]	(2.7)	(0.0)	(0.0)	(0.0)	(1.5)	(0.4)	(0.0)	(4.8)
PMB30-adsorbed Co–Cr–Mo	70.6	24.1	2.3	3.0	0.0	0.0	0.0	0.0	95.8[b]
	(1.4)	(1.3)	(0.4)	(0.3)	(0.0)	(0.0)	(0.0)	(0.0)	(3.5)
PMSi90-immobilized Co–Cr–Mo	61.4	29.5	3.6	4.2	1.3	0.1	0.0	0.0	16.6[b]
	(0.9)	(0.7)	(0.4)	(0.1)	(0.4)	(0.2)	(0.0)	(0.0)	(2.4)
PMPC-grafted Co–Cr–Mo	61.7	28.0	5.0	5.3	0.1	0.0	0.0	0.0	23.5[b]
	(0.7)	(0.6)	(0.3)	(0.1)	(0.1)	(0.0)	(0.0)	(0.0)	(8.4)

[a] The standard deviations are shown in parentheses.
[b] Significant difference ($p < 0.001$) as compared to the untreated Co–Cr–Mo.

2.11. Statistical analysis

The results derived from each measurement in the water-contact angle measurement, friction test, and protein adsorption test were expressed as mean values ± standard deviation. The statistical significance ($p < 0.05$) was estimated by Student's *t*-test.

3. Results

Fig. 2 shows the FT-IR/ATR spectra of the surface-modified Co–Cr–Mo samples with various MPC polymers. Absorption peaks were newly observed for the surface-modified Co–Cr–Mo with MPC polymers. The peaks at 1720, 1550, and 1460 cm^{-1} are attributed to C = O and -CH_2- in the MPC polymer. The peaks at 1180, 1040, 700, and 630 cm^{-1} are attributed to the trimethoxysilane group in the MPSi unit [19]. The peaks at 1240, 1080, 970, and 920 cm^{-1} are attributed to the $-N^+(CH_3)_3$ and phosphate groups in the MPC unit [22]. The absorption peak intensities of the phosphate groups of the

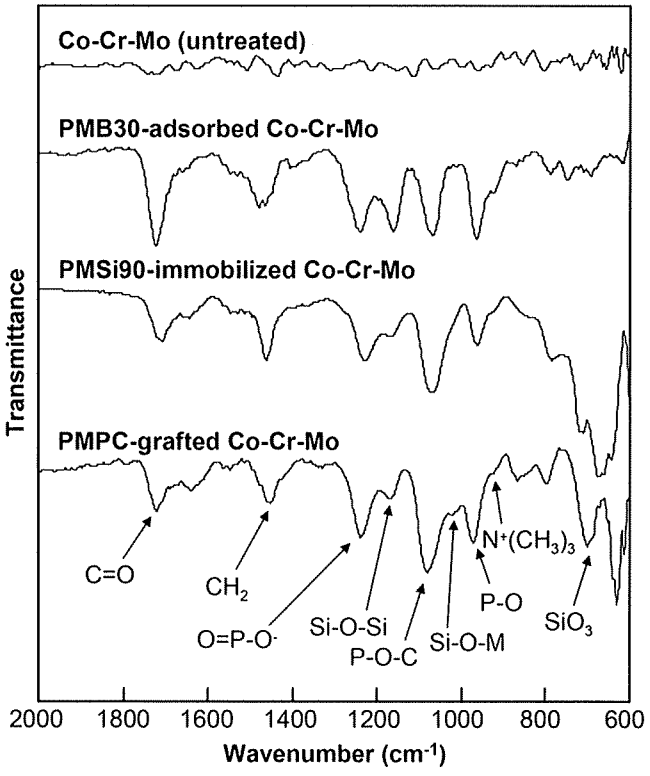

Fig. 2. FT-IR/ATR spectra of untreated Co–Cr–Mo, MPC polymer-coated Co–Cr–Mo, and PMPC grafted Co–Cr–Mo.

PMPC-grafted Co–Cr–Mo were the highest in the Co–Cr–Mo whose surface was modified by the MPC polymer.

Table 1 summarizes the surface elemental composition and static-water contact angle of the surface-modified Co–Cr–Mo samples with various MPC polymers. The nitrogen (N) and phosphorous (P) contents in all the Co–Cr–Mo samples whose surfaces were modified by the MPC polymer were observed. The elemental compositions of both N and P in the surface-modified Co–Cr–Mo increased with an increase in the MPC composition in the polymer for surface modification. In particular, these values of N and P in the PMPC-grafted Co–Cr–Mo surface were 5.0 and 5.3 atom%, respectively, and were almost equivalent to the theoretical elemental composition (N = 5.3, P = 5.3 atom%) of PMPC. The static-water contact angle of the untreated Co–Cr–Mo was 81.6°, and this decreased markedly to approximately 20° (i.e., 16.6°–23.5°, $p < 0.001$) by the modifications with PMSi90 and PMPC.

Fig. 3 shows the cross-sectional TEM images of the surface-modified Co–Cr–Mo samples with various MPC polymers. For PMB30-adsorption, PMSi90-immobilization, and PMPC-grafting, a thickness of 50, 130, and 200 nm, respectively, of the MPC polymer layers was clearly observed on the surface of the Co–Cr–Mo substrate. No cracks due to poor adhesion and/or delamination were observed at the interface between the MPC polymer layer and Co–Cr–Mo substrate. These results indicate that each surface modification layer on the Co–Cr–Mo substrate is uniform and adheres closely, regardless of the binding conditions; the surface modification layers by PMB30-adsorption, PMSi90-immobilization, and PMPC-grafting combine with the substrate by physical adsorption and covalent bonds of Si–O–metal (M), respectively. However, in the PMB30-adsorbed Co–Cr–Mo, a bilayer structure for poor adhesion attributed to dipping twice was clearly observed on the surface modification layer. Further, in the PMB30-adsorbed and PMSi90-immobilized Co–Cr–Mo samples, a porous structure was clearly observed on the surface modification layer. This porous structure was also observed on the surface modification layer prepared by the slow-rate solvent evaporation method (approximately for 1 month at 4 °C, data not shown).

Fig. 4 shows the EDX spectra of the surface-modified Co–Cr–Mo samples with various MPC polymers. In spectra (b_{1-3}), (c_{1-3}), and (d_{1-3}) of the MPC polymer layers, a significant peak attributed to the P atom was observed at 2.0 keV. This peak is mainly attributed to the MPC units. Interestingly, this peak was clearly observed in spectra (b_2) and (c_2) of the porous part of the MPC polymer layer. In spectra (c_1) and (d_1) of the interface of the PMSi90-immobilization layer and the intermediate layer of the PMPC-grafted Co–Cr–Mo, peaks were observed at 0.5 and 1.7 keV. These peaks are attributed to the O and Si atoms in the interface/intermediate layer between the silane of the MPSi and the metal oxide of the Co–Cr–Mo.

Fig. 5 shows the amounts of BSA, γ-globulins, and fibrinogen adsorbed on the surface-modified Co–Cr–Mo samples with various

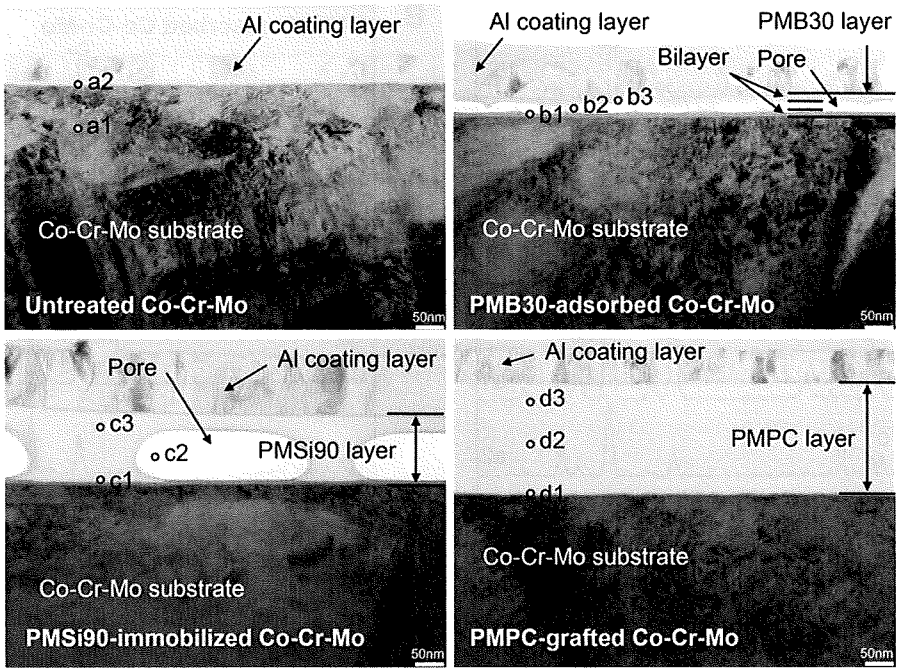

Fig. 3. Cross-sectional TEM images of the surface-modified Co–Cr–Mo with various MPC polymers. Aluminum coating layers (approximately 70–100 nm) for the preparation of TEM observation specimen are shown above the MPC polymer layer of the Co–Cr–Mo surface. Small open circles indicate EDX analysis points. Bar: 50 nm.

MPC polymers. The amount of each protein adsorbed on the Co–Cr–Mo surface modified by the MPC polymer was considerably lower ($p < 0.001$) than that on the untreated Co–Cr–Mo. These results imply that the surface modification by the MPC polymer results in good biocompatibility.

Fig. 6 shows the coefficients of dynamic friction of the sliding couples and articular cartilage pins sliding against the surface-modified Co–Cr–Mo plates with various MPC polymers. The PMB30-adsorbed and PMSi90-immobilized Co–Cr–Mo samples showed a slightly higher friction coefficient than the untreated Co–Cr–Mo sample in water at room temperature (not significantly different); in contrast, the MPC polymer-coated Co–Cr–Mo showed a lower friction coefficient than the untreated Co–Cr–Mo in BS mixture at 37 °C ($p < 0.05$). Further, the friction coefficient of the PMPC-grafted Co–Cr–Mo decreased drastically compared with untreated Co–Cr–Mo ($p < 0.001$) and reached approximately <0.010 in both lubricant conditions, i.e., water at room temperature and the BS mixture at 37 °C; moreover, it remained almost steady. The friction coefficients of all MPC polymer-containing BS mixtures were drastically lower as compared with that of non-additive BS mixture (Fig. 6).

Fig. 7 shows the coefficients of dynamic friction of the untreated Co–Cr–Mo and PMPC-grafted Co–Cr–Mo samples as a function of the loads. At both 10 and 100 cycles, the PMPC-grafted Co–Cr–Mo sample showed a remarkably low friction coefficient of approximately 0.019 at a load of 0.49 N; this value decreased gradually and reached approximately <0.010 at a load of 9.80 N. Similarly, the friction coefficients of the untreated Co–Cr–Mo sample in the initial 10 cycles decreased gradually from 0.188 to 0.045. However, this value of the untreated Co–Cr–Mo at 100 cycles decreased to 0.082 up to loads of 1.96 N; it then gradually increased with an increase in the loads. Fig. 7B shows the friction coefficients of the untreated Co–Cr–Mo and PMPC-grafted Co–Cr–Mo samples as a function of the test durations. It was observed that the friction coefficient was significantly lower in the PMPC-grafted Co–Cr–Mo sample than in the untreated Co–Cr–Mo one. This value was almost constant throughout the 5×10^3 cycles of the friction test.

Fig. 8 shows the histological findings of the articular cartilage pins after 5×10^3 cycles of friction tests. In the cartilage against the untreated Co–Cr–Mo, the cartilage layer of the worn surface became thicker as compared with the surrounding articular cartilage of the unworn surface. In contrast, in the cartilage against the PMPC-grafted Co–Cr–Mo, the layer of the worn surface did not differ considerably from that of the unworn surface.

Fig. 9 shows the time course of the surface modification layer of the untreated, MPC polymer-coated, and PMPC-grafted Co–Cr–Mo samples during PBS soaking. The elemental compositions of both N and P in the untreated, PMB30-adsorbed, and PMPC-grafted Co–Cr–Mo samples were almost constant throughout the 12 weeks of PBS soaking. In contrast, in the PMSi90-immobilized Co–Cr–Mo sample, these values decreased gradually with the PBS-soaking duration. Similarly, the static-water contact angle of untreated, PMB30-adsorbed, and PMPC-grafted Co–Cr–Mo samples were almost constant throughout PBS soaking, whereas the values in PMSi90-immobilized Co–Cr–Mo increased gradually.

Fig. 10 shows FM images of the surface-modified Co–Cr–Mo samples with various MPC polymers before and after friction tests/PBS-soaking tests. After 100 cycles of friction tests, the MPC polymer layer was removed from the PMB30-adsorbed and PMSi90-immobilized Co–Cr–Mo sliding surfaces; in contrast, most of the PMPC-grafted Co–Cr–Mo sliding surface was covered by the PMPC layer. After 12 weeks of PBS-soaking tests, most of the MPSi90 layer was removed from the Co–Cr–Mo surface, while most of the PMB30-adsorbed and PMPC-grafted Co–Cr–Mo surface was covered stably by the MPC polymer layer.

4. Discussion

In the hemi-arthroplasty, the highly lubricious surface by a "mild treatment" with soft materials was requested with aim of preserving the degradation of the articular cartilage. In this study, we have prepared various surface modification layers formed on the Co–Cr–Mo surface by MPC polymer coating or photoinduced radical polymerization of MPC to form PMPC graft chains for

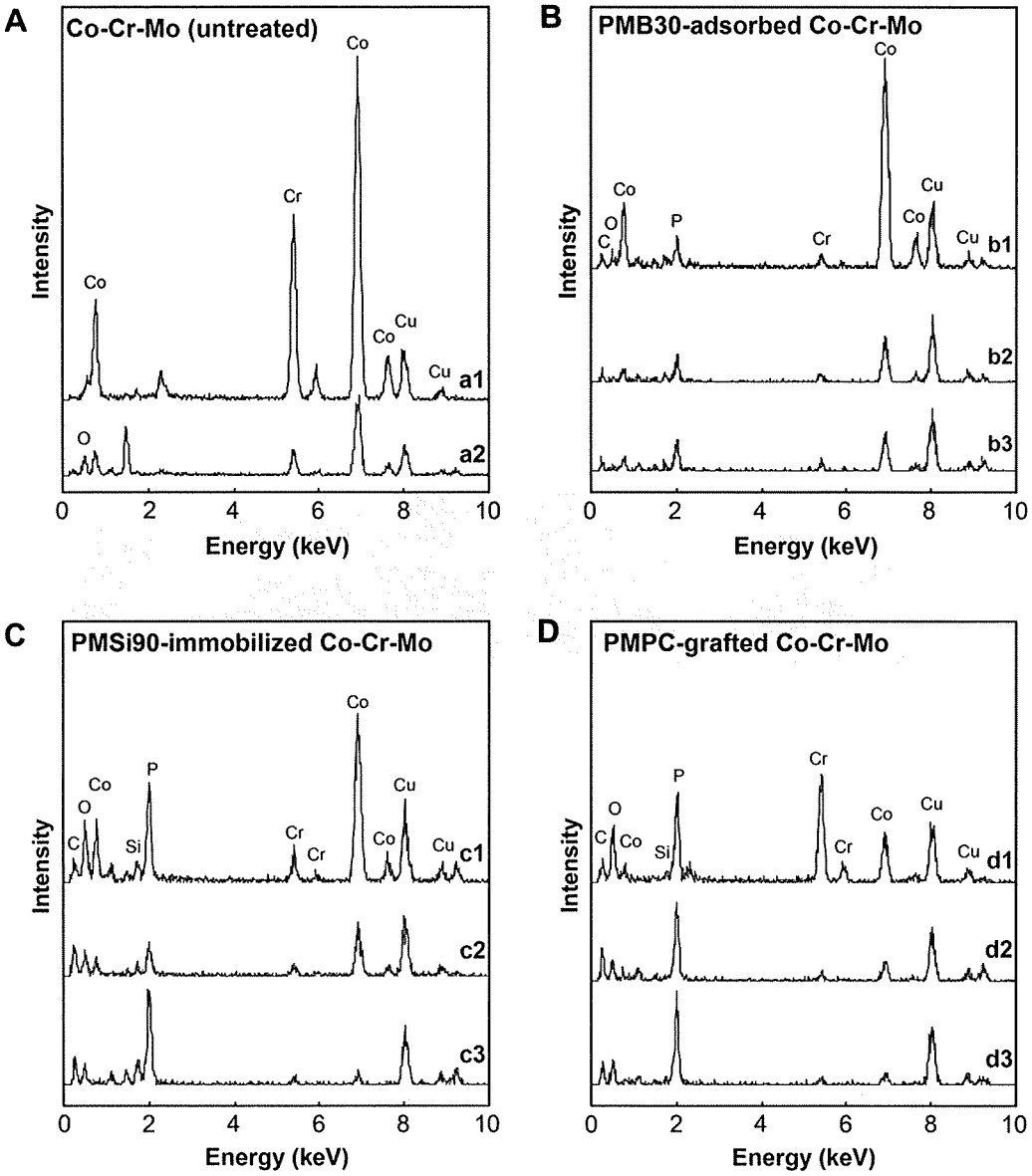

Fig. 4. EDX spectra of the untreated Co–Cr–Mo, MPC polymer-coated Co–Cr–Mo, and PMPC-grafted Co–Cr–Mo. The spectra were analyzed on the cross-section (small open circles in Fig. 3) of the untreated Co–Cr–Mo, MPC polymer-coated Co–Cr–Mo, and PMPC-grafted Co–Cr–Mo.

improving lubrication and preventing the degradation of acetabular cartilage. Here, we discuss the structures and stabilities of the surface modification layers of the MPC polymer and the effects of these characteristics on the retention of articular cartilage in hemiarthroplasty.

To ensure the *in vivo* long-term stability of the MPC modified layer on the Co–Cr–Mo surface, it is necessary to create strong covalent bonding between the Co–Cr–Mo substrate and the MPC polymer. Organosilanes have already been known as surface coupling agents that enhance bonding between a metal or a metal oxide surface and an organic resin such as dental resin; moreover, they can strongly bind metals to resins in dental implants [23]. Organic silanes or silane coupling agents comprise at least a hydrolyzable alkoxysilyl or chlorosilyl group and an organofunctional group. The agents are effective for introducing organofunctional groups into the siloxane network polymer. The organofunctional group in the silane could be useful for improving bonding with the organic overlayer. MPSi binds to the Co–Cr–Mo substrate by a condensation reaction in two steps; in the first step, MPSi is hydrolyzed (activated) and in the second step, the hydrolyzed silane molecule binds to the surface by an Si–O–M bond, forming branched hydrophobic siloxane bonds, i.e., Si–O–Si. The hydrolyzed silane molecule has three –OH groups that can react with the –OH groups of the surface metallic oxide layer to form siloxane bonds covalently. The peaks at 1180 and 1040 cm^{-1} in the FT-IR/ATR spectrum of the PMSi90-immobilized and PMPC-grafted Co–Cr–Mo surfaces were attributed to Si–O–Si and Si–O–M, respectively (Fig. 2).

However, several previous studies have reported that a silane coating has low water resistance due to hydrolysis of the siloxane bond and desorption of the physisorbed silane [24]. In fact, the PMSi90-immobilization layer was removed from the Co–Cr–Mo surface after 12 weeks of PBS soaking (Figs. 9 and 10). Zhang, et al. and others have reported that the water stability of Si–O–M could be improved by employing the following factors: (1) an induction of bridged silane coupling agents, when hydrolyzed, contain two or more $-Si(OH)_3$, (2) the hydrophobic alkyl moieties that limit the contact with water, and (3) an increase in the thickness of the

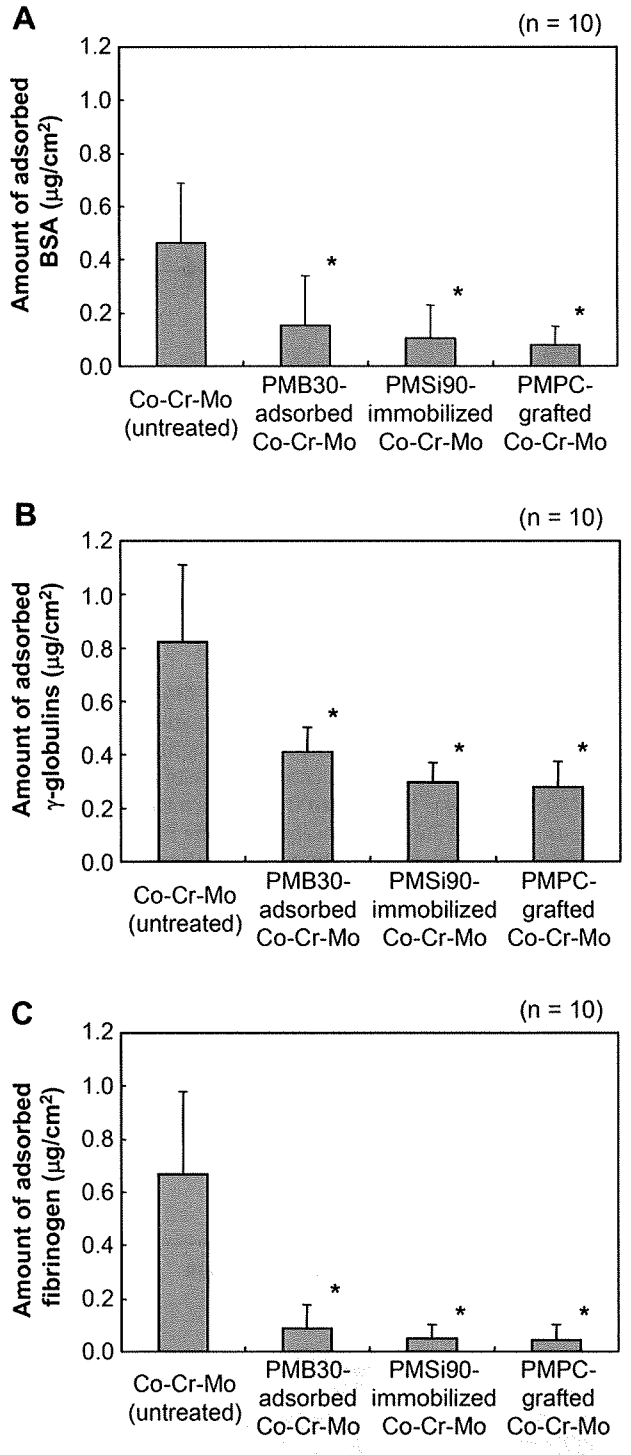

Fig. 5. Amounts of (A) BSA, (B) γ-globulins, and (C) fibrinogen adsorbed on the surfaces of the untreated Co–Cr–Mo, MPC polymer-coated Co–Cr–Mo, and PMPC-grafted Co–Cr–Mo. Bar: Standard deviations. *: Significant difference ($p < 0.001$) as compared to the untreated Co–Cr–Mo.

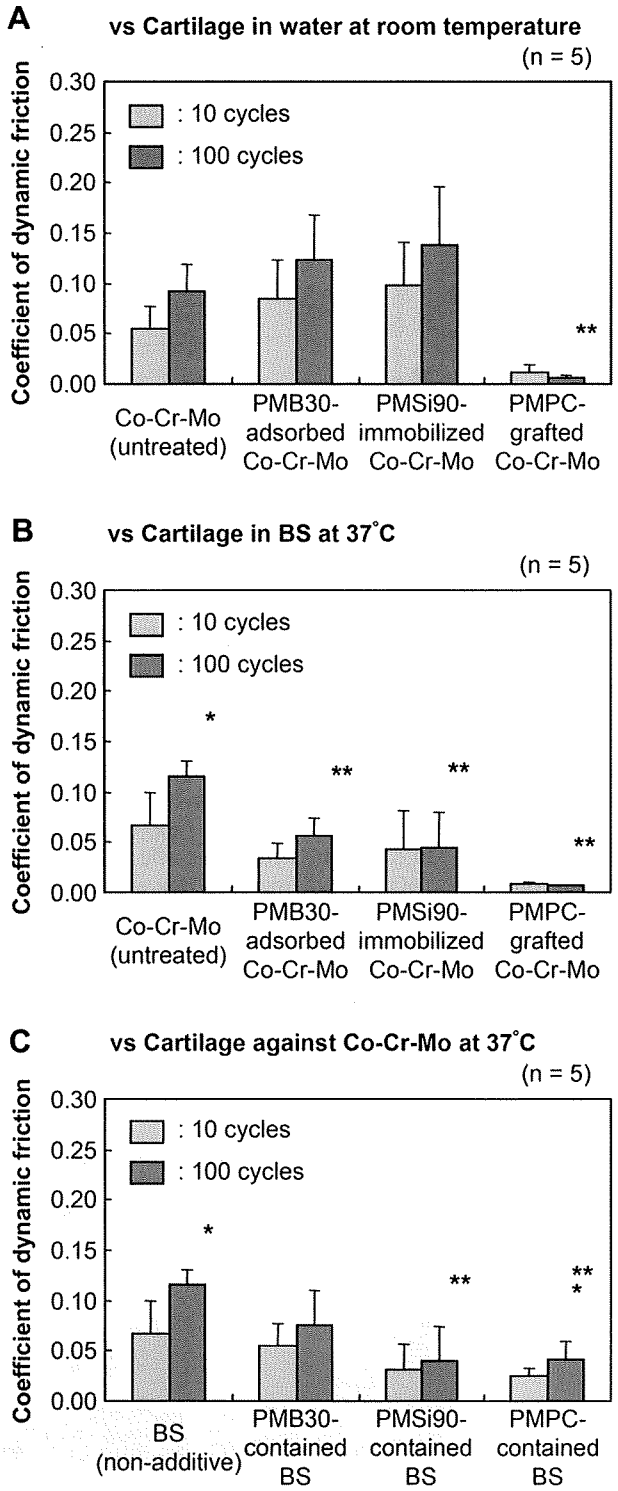

Fig. 6. Coefficients of dynamic friction of the untreated, MPC polymer-coated, and PMPC-grafted Co–Cr–Mo in the pin-on-plate friction test with various lubrication conditions. (A) Against cartilage pin with water at room temperature, (B) against cartilage pin with BS lubricant at 37 °C, (C) untreated Co–Cr–Mo plate against cartilage pin with BS lubricant with MPC polymer as additive at 37 °C. Bar: Standard deviations. *: *t*-test, significant difference ($p < 0.05$) as compared to the coefficients of dynamic friction at 10 cycles, and **: *t*-test, significant difference ($p < 0.05$) as compared to the untreated Co–Cr–Mo plate at 100 cycles.

surface oxide layer [25]. Therefore, it was considered that the MPSi intermediate layer with a bridge of three methoxysilane groups with MPSi unit composition of 100% (MPSi unit of PMSi90 composition was 10% only) was essential in PMPC-grafted Co–Cr–Mo. Additionally, a functional methacrylate and pretreatment (nitric acid treatment and O_2 plasma treatment) for the Co–Cr–Mo surface were used. As shown in Figs. 9 and 10, the high stability of

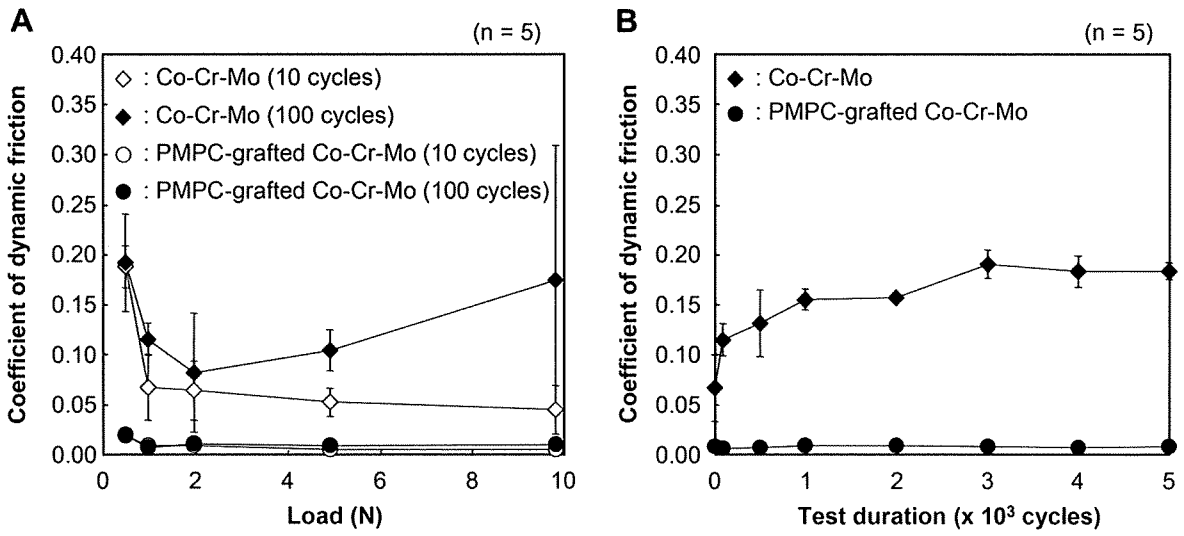

Fig. 7. Coefficients of dynamic friction of the untreated and PMPC-grafted Co–Cr–Mo in the pin-on-plate friction test. (A) Coefficients of dynamic friction of the untreated and PMPC-grafted Co–Cr–Mo against cartilage pin as a function of loads in the pin-on-plate friction test with BS lubricant at 37 °C. (B) Time course of coefficients of dynamic friction of the untreated and PMPC-grafted Co–Cr–Mo against the cartilage pin during 5×10^3 cycles of loading with 0.98 N in the pin-on-plate friction test with BS lubricant at 37 °C. Bar: Standard deviations.

the PMPC-grafted layer was confirmed throughout 12 weeks of PBS soaking.

On the other hand, the high stability of the PMB30-adsorbed layer was also confirmed throughout 12 weeks of PBS soaking. As shown in Table 1, the static-water contact angle of the PMB30-adsorbed Co–Cr–Mo was 95.8°. Sibarani et al. reported that the PMB30-adsorbed polymer surfaces showed high advancing (approximately 100°) and low receding (approximately 20°) contact angles: PMB30 cannot be hydrated easily due to the low MPC unit composition of the copolymer [10]. However, as shown in Fig. 5, the PMB30-adsorbed Co–Cr–Mo surface, which could form a phosphorylcholine-enriched surface after equilibrating for 1 h, showed excellent biocompatibility as an anti-protein adsorption surface. Hence, the PMB30-adsorbed layer has been observed to be stable (insoluble and attachable *in vivo* condition) and useful on several medical devices [14,15].

In Figs. 6 and 7, the PMPC-grafted Co–Cr–Mo surface shows an extremely low friction coefficient as compared to that of the untreated Co–Cr–Mo surface. Since MPC is highly hydrophilic and PMPC is water soluble, the water contact angle of the PMPC-grafted Co–Cr–Mo surface was lower than that of the untreated Co–Cr–Mo surface, as shown in Table 1. Consequently, the PMPC-grafted layer successfully provided high lubricity in the form of "surface gel hydration lubrication" to the Co–Cr–Mo surface (Fig. 3). A previous study has reported that the hydrogel cartilage surface is assumed to have a brush-like structure: a part of the proteoglycan brush is bonded with the collagen network on the cartilage surface [26]. The bearing surface with PMPC is assumed to have a brush-like structure similar to that of articular cartilage. Cartilage/PMPC-grafted Co–Cr–Mo bearing couples can therefore be regarded to be mimicking natural joint cartilage *in vivo*. The friction coefficient of cartilage/cartilage was reported to be approximately 0.01–0.02

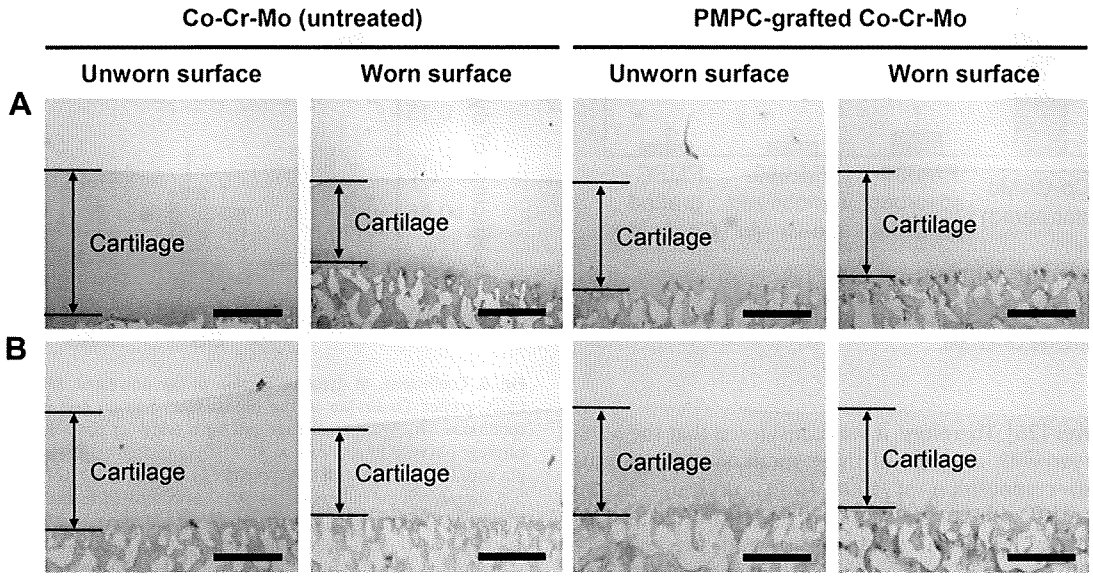

Fig. 8. Histological findings of the articular cartilage pins after 5×10^3 cycles of friction tests. (A) H&E stained, and (B) safranin-O stained. Bar; 500 μm.

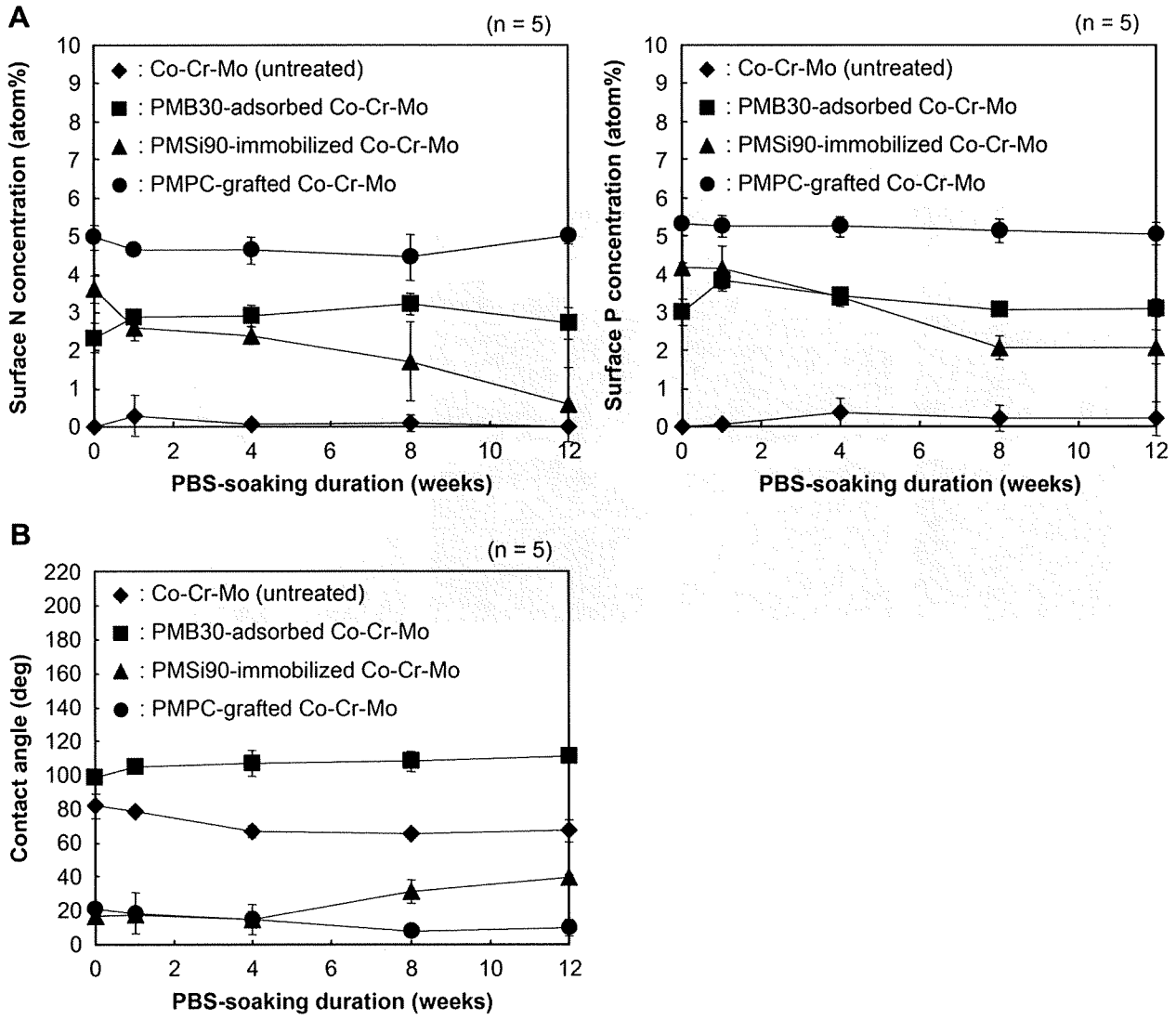

Fig. 9. Time course of the surface-modification layer of the untreated, MPC polymer-coated and PMPC-grafted Co–Cr–Mo during PBS soaking with 120 rpm shaking at 37 °C. (A) Surface N and P concentrations by XPS, and (B) static-water contact angle. Bar: Standard deviations.

[27,28]. In this study, it was found that the cartilage/PMPC-grafted Co–Cr–Mo interface mimicking a natural joint showed low friction (friction coefficient was <0.01), i.e., as low as that of cartilage/cartilage interface. Hence, it was considered that the PMPC-grafted Co–Cr–Mo surface is well suited for application on the artificial femoral head that would chafe against articulating cartilage. We expect that hemi-arthroplasty with a PMPC-grafted Co–Cr–Mo femoral head will be a promising option that preserves acetabular cartilage and extends the duration before total hip arthroplasty (THA) in young patients. Moreover, we consider that these effects would occur continuously. In Fig. 7B, the friction coefficient shows a test duration-dependent response for articular cartilage against the untreated Co–Cr–Mo sample due to the continued loading of the cartilage tissue and the ensuing loss of fluid-film formation (or rehydration). It was thought that the thickness of the cartilage tissue atrophied due to the fairly poor access of the cartilage tissue to water (Fig. 8). Decreased water content often leads to the degradation of cartilage function. Although cartilage tissues are able to produce matrix components throughout life, i.e., carry out regeneration, their production cannot keep pace with the repair requirements after acute damage to articular cartilage; such damages limit the longevity of the artificial femoral head and its stability after hemi-arthroplasty. In contrast, in articular cartilage against the PMPC-grafted Co–Cr–Mo sample, the friction coefficient remained at a steady low value due to the rehydration of the continuously loaded cartilage tissue, and the articular cartilage surface was preserved.

In Fig. 6A, the PMB30-adsorbed and PMSi90-immobilized Co–Cr–Mo samples show a slightly higher friction coefficient than the untreated Co–Cr–Mo sample in water at room temperature. Some pores in the PMB30 and PMSi90 layers on the Co–Cr–Mo surface could be observed (Fig. 3); these may have occurred due to the low density of the material because physical adsorption or chemical immobilization of the polymer was used as the surface modification method. Therefore, it is assumed that a sliding couple with cartilage and low-density MPC polymer layer may cause high friction by stick-slip motion with interpenetration [18]. Furthermore, the MPC polymer-coated Co–Cr–Mo showed a lower friction coefficient than the untreated Co–Cr–Mo in BS mixture at 37 °C (Fig. 6B). It was thought that the interpenetration of cartilage and low-density MPC polymer layer was blocked by the protein of BS presented between the interfaces. In contrast, the friction coefficient of the PMPC-grafted Co–Cr–Mo sample was drastically as compared with that of the untreated Co–Cr–Mo sample; the degree

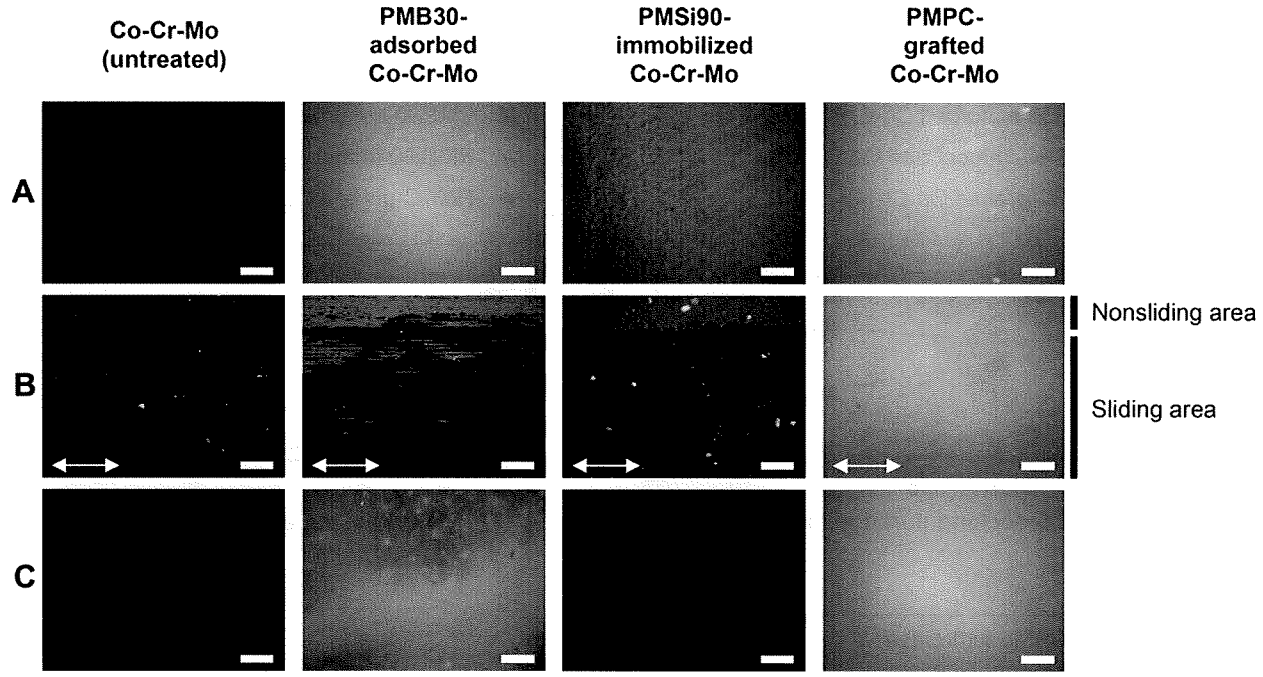

Fig. 10. FM images of the untreated Co–Cr–Mo, MPC polymer-coated Co–Cr–Mo, and PMPC-grafted Co–Cr–Mo surfaces. FM images of the surface before tests (A), after 100 cycles of friction tests with BS lubricant (B), and after 12 weeks of PBS-soaking tests (C). Bar; 200 μm. Arrow; Sliding direction of friction test.

of reduction in the coefficient was 93%. PMPC-grafted Co–Cr–Mo might have a high density because the polymerization method used was surface-initiated graft polymerization, termed as the "grafting from" method [19,29]. A sliding couple with cartilage tissue and high-density PMPC layer fabricated by the "grafting from" method may be responsible for low friction, such as that in the case of "super-lubricity," because of resistance to interpenetration by volume effects resulting from the mobility of hydrophilic macromolecules of cartilage tissue and the PMPC-grafted layer [30–32].

As shown in Fig. 7A, the friction coefficients of the articular cartilage against the untreated and PMPC-grafted Co–Cr–Mo samples decreased with an increasing load in the initial 10 cycles. The elastic articular cartilage tissue and PMPC-grafted layer was slightly deformed by the loads; the low friction coefficient might occur in order to increase the contact area of the fluid film's concave surface. However, the friction coefficient of the articular cartilage against the untreated Co–Cr–Mo at 100 cycles decreased to 0.082 up to loads of 1.96 N; a further increase in loads up to 9.8 N resulted in elevated friction coefficients. Under a high load, water exudes slowly from the articular cartilage with sliding [27]. As the result of water loss, the thickness of the surface layer and/or fluid film reduces, and the water content of the surface-hydration layer decreases. Consequently, the degree of adhesion of articular cartilage to the Co–Cr–Mo surface increases due to a lack of rehydration and because of the increase in frictional force. In contrast, the PMPC-grafted Co–Cr–Mo sample at 100 cycles showed a remarkably low friction coefficient that reached approximately <0.010 at a load of 9.80 N. We consider that this result implies that the rehydration and hydrodynamic lubrication mechanism of the articular cartilage is supported by the hydrated PMPC-grafted layer, similar to the interface between cartilage/cartilage of the natural joint.

The friction coefficients of cartilage/untreated Co–Cr–Mo interface with all MPC polymer-containing BS mixtures as a lubricant were drastically lower as compared with that with the non-additive BS mixture (Fig. 6C). Synovial fluid as a whole, and all its components such as hyaluronic acid, glycoprotein (mainly lubricin), and surface-active phospholipids, have been proposed as lubricants responsible for boundary lubrication in the natural joint [33]. Similarly, it is considered that the additives of MPC polymer would play the role akin to synovial phospholipids for boundary lubrication, and the adsorption of the MPC polymer to the sliding surface could prevent direct contact between the cartilage and the untreated Co–Cr–Mo and hence decrease the frictional force between them. However, in the case of additives, the lubricity may change depending on the ambient *in vitro* and *in vivo* conditions, because the additives probably diffuse to synovial fluid *in vivo*.

The amounts of the representative protein, BSA, γ-globulins, and fibrinogen, adsorbed on the modified Co–Cr–Mo surface with the MPC polymer were significantly low, these reached to 7%–50% of that of the untreated surface, as shown in Fig. 5. It is hypothesized that the mechanism underlying protein adsorption resistivity of a surface modified by the MPC polymer is based on the water structure resulting from the interactions between water molecules and phosphorylcholine groups [34]. The large amount of free water around the phosphorylcholine group is considered to detach proteins easily and prevent conformational changes in the adsorbed proteins even when the proteins attached to the surface [3,34]. The reduction in protein adsorption is also considered to be caused by the presence of a hydrated layer around the phosphorylcholine group [35]. The latter consideration is consistent with the results of the water contact angle measurement, friction test, and TEM and FM observations of the Co–Cr–Mo samples whose surfaces were modified by the MPC polymer. It should be noted that the porous structure (low density) of the PMB30-adsorption and PMSi90-immobilization layer (in dry conditions) hardly affected the protein adsorption. Therefore, the Co–Cr–Mo sample whose surface is modified by the MPC polymer is expected to exhibit tissue and blood compatibility, i.e., biocompatibility, because previous studies have reported that the MPC polymer-modified surfaces exhibit *in vivo* biocompatibility [6–16].

5. Conclusions

In this study, we systematically investigated the surface properties of the various surface modification layers formed on the Co–Cr–Mo surface by the MPC polymer by dip coating or photoinduced radical grafting. We conclude that several important issues are involved in the long-term retention of the benefits of the MPC polymer used in artificial joints under variable and multidirectional loads, for example, strong bonding between the MPC polymer and the Co–Cr–Mo surface as also a high density of the MPC polymer. We suggest that the MPSi intermediate layer and photoinduced radical graft polymerization should be employed to create strong covalent bonding between the surface modification layer and Co–Cr–Mo substrate and to retain the high density of the polymer chains of that layer. The cartilage/PMPC-grafted Co–Cr–Mo interface, which mimicked a natural joint, showed an extremely low friction coefficient of <0.01, a value as low as that of a natural cartilage interface. We expect that the PMPC-grafted Co–Cr–Mo femoral head for hemi-arthroplasty will be a promising option for preserving acetabular cartilage and extending the duration before THA.

Acknowledgements

This study was supported by the Health and Welfare Research Grant for Translational Research (H17-005), Research on Medical Devices for Improving Impaired QOL (H20-004) from the Japanese Ministry of Health, Labour and Welfare. We thank Mr. Y. Yoshihara and Ms. Y. Nakao, Japan Medical Materials Corporation, for their excellent technical assistance.

Appendix

Figures with essential colour discrimination. Certain figures in this article, in particular Figures 8 and 10, are difficult to interpret in black and white. The full colour images can be found in the on-line version, at doi:10.1016/j.biomaterials.2009.09.083.

References

[1] Healy WL, Lemos DW, Appleby D, Lucchesi CA, Saleh KJ. Displaced femoral neck fractures in the elderly: outcomes and cost effectiveness. Clin Orthop Relat Res 2001;383:229–42.
[2] Beaulé PE, Amstutz HC, Le Duff M, Dorey F. Surface arthroplasty for osteonecrosis of the hip: hemiresurfacing versus metal-on-metal hybrid resurfacing. J Arthroplasty 2004;19(8 Suppl. 3):54–8.
[3] Kyomoto M, Moro T, Miyaji F, Hashimoto M, Kawaguchi H, Takatori Y, et al. Effects of mobility/immobility of surface modification by 2-methacryloyloxyethyl phosphorylcholine polymer on the durability of polyethylene for artificial joints. J Biomed Mater Res A 2009;90(2):362–71.
[4] Kyomoto M, Moro T, Miyaji F, Hashimoto M, Kawaguchi H, Takatori Y, et al. Effect of 2-methacryloyloxyethyl phosphorylcholine concentration on photoinduced graft polymerization of polyethylene in reducing the wear of orthopaedic bearing surface. J Biomed Mater Res A 2008;86(2):439–47.
[5] Kyomoto M, Moro T, Miyaji F, Konno T, Hashimoto M, Kawaguchi H, et al. Enhanced wear resistance of orthopedic bearing due to the cross-linking of poly(MPC) graft chains induced by gamma-ray irradiation. J Biomed Mater Res B Appl Biomater 2008;84(2):320–7.
[6] Moro T, Takatori Y, Ishihara K, Konno T, Takigawa Y, Matsushita T, et al. Surface grafting of artificial joints with a biocompatible polymer for preventing periprosthetic osteolysis. Nature Mater 2004;3:829–37.
[7] Moro T, Takatori Y, Ishihara K, Nakamura K, Kawaguchi H. 2006 Frank Stinchfield Award: grafting of biocompatible polymer for longevity of artificial hip joints. Clin Orthop Relat Res 2006;453:58–63.
[8] Moro T, Kawaguchi H, Ishihara K, Kyomoto M, Karita T, Ito H, et al. Wear resistance of artificial hip joints with poly(2-methacryloyloxyethyl phosphorylcholine) grafted polyethylene: comparisons with the effect of polyethylene cross-linking and ceramic femoral heads. Biomaterials 2009;30(16):2995–3001.
[9] Kyomoto M, Ishihara K. Self-initiated surface graft polymerization of 2-methacryloyloxyethyl phosphorylcholine on poly(ether–ether–ketone) by photo-irradiation. ACS Appl Mater Interfaces 2009;1(3):537–42.
[10] Sibarani J, Takai M, Ishihara K. Surface modification on microfluidic devices with 2-methacryloyloxyethyl phosphorylcholine polymers for reducing unfavorable protein adsorption. Colloids Surf B Biointerfaces 2007;54(1):88–93.
[11] Ueda T, Oshida H, Kurita K, Ishihara K, Nakabayashi N. Preparation of 2-methacryloyloxyethyl phosphorylcholine copolymers with alkyl methacrylates and their blood compatibility. Polym J 1992;24(11):1259–69.
[12] Konno T, Ishihara K. Temporal and spatially controllable cell encapsulation using a water-soluble phospholipid polymer with phenylboronic acid moiety. Biomaterials 2007;28(10):1770–7.
[13] Xu Y, Takai M, Konno T, Ishihara K. Microfluidic flow control on charged phospholipid polymer interface. Lab Chip 2007;7(2):199–206.
[14] Snyder TA, Tsukui H, Kihara S, Akimoto T, Litwak KN, Kameneva MV, et al. Preclinical biocompatibility assessment of the EVAHEART ventricular assist device: coating comparison and platelet activation. J Biomed Mater Res A 2007;81(1):85–92.
[15] Ueda H, Watanabe J, Konno T, Takai M, Saito A, Ishihara K. Asymmetrically functional surface properties on biocompatible phospholipid polymer membrane for bioartificial kidney. J Biomed Mater Res A 2006;77(1):19–27.
[16] Kyomoto M, Moro T, Konno T, Takadama H, Yamawaki N, Kawaguchi H, et al. Enhanced wear resistance of modified cross-linked polyethylene by grafting with poly(2-methacryloyloxyethyl phosphorylcholine). J Biomed Mater Res A 2007;82(1):10–7.
[17] Ishihara K, Ueda T, Nakabayashi N. Preparation of phospholipid polymers and their properties as polymer hydrogel membranes. Polym J 1990;22(5):355–60.
[18] Kyomoto M, Iwasaki Y, Moro T, Konno T, Miyaji F, Kawaguchi H, et al. High lubricious surface of cobalt–chromium–molybdenum alloy prepared by grafting poly(2-methacryloyloxyethyl phosphorylcholine). Biomaterials 2007;28(20):3121–30.
[19] Kyomoto, M., Moro, T., Iwasaki, Y., Miyaji, F., Kawaguchi, H., Takatori, Y., et al. Superlubricious surface mimicking articular cartilage by grafting poly(2-methacryloyloxyethyl phosphorylcholine) on orthopaedic metal bearings. J Biomed Mater Res A, in press.
[20] Wang JH, Bartlett JD, Dunn AC, Small S, Willis SL, Driver MJ, et al. The use of rhodamine 6G and fluorescence microscopy in the evaluation of phospholipid-based polymeric biomaterials. J Microsc 2005;217(Pt 3):216–24.
[21] Arendt SA, Bailey SJ, editors. ASTM F732–00: standard test method for wear testing of polymeric materials used in total joint prostheses. Annual book of ASTM standards, vol. 13; 2004.
[22] Kyomoto M, Moro T, Konno T, Takadama H, Kawaguchi H, Takatori Y, et al. Effects of photo-induced graft polymerization of 2-methacryloyloxyethyl phosphorylcholine on physical properties of cross-linked polyethylene in artificial hip joints. J Mater Sci Mater Med 2007;18:1809–15.
[23] Yoshida K, Greener EH. Effects of coupling agents on mechanical properties of metal oxide-polymethacrylate composites. J Dent 1994;22:57–62.
[24] Matinlinna JP, Vallittu PK. Bonding of resin composites to etchable ceramic surfaces – an insight review of the chemical aspects on surface conditioning. J Oral Rehabil 2007;34(8):622–30.
[25] Zhang Z, Berns AE, Willbold S, Buitenhuis J. Synthesis of poly(ethylene glycol) (PEG)-grafted colloidal silica particles with improved stability in aqueous solvents. J Colloid Interface Sci 2007;310(2):446–55.
[26] Ishikawa Y, Hiratsuka K, Sasada T. Role of water in the lubrication of hydrogel. Wear 2006;261:500–4.
[27] Katta J, Jin Z, Ingham E, Fisher J. Biotribology of articular cartilage – a review of the recent advances. Med Eng Phys 2008;30(10):1349–63.
[28] Bell CJ, Ingham E, Fisher J. Influence of hyaluronic acid on the time-dependent friction response of articular cartilage under different conditions. Proc Inst Mech Eng [H] 2006;220(1):23–31.
[29] Matsuda T, Kaneko M, Ge S. Quasi-living surface graft polymerization with phosphorylcholine group(s) at the terminal end. Biomaterials 2003;24:4507–15.
[30] Raviv U, Glasson S, Kampf N, Gohy JF, Jérôme R, Klein J. Lubrication by charged polymers. Nature 2003;425:163–5.
[31] Chen M, Briscoe WH, Armes SP, Klein J. Lubrication at physiological pressures by polyzwitterionic brushes. Science 2009;323(5922):1698–701.
[32] Kobayashi M, Terayama Y, Hosaka N, Kaido M, Suzuki A, Yamada N, et al. Friction behavior of high-density poly(2-methacryloyloxyethyl phosphorylcholine) brush in aqueous media. Soft Matter 2007;2:740–6.
[33] Sawae Y, Yamamoto A, Murakami T. Influence of protein and lipid concentration of the test lubricant on the wear of ultra high molecular weight polyethylene. Tribol Int 2008;41(7):648–56.
[34] Goda T, Konno T, Takai M, Ishihara K. Photoinduced phospholipid polymer grafting on Parylene film: advanced lubrication and antibiofouling properties. Colloids Surf B Biointerfaces 2007;54(1):67–73.
[35] Hoshi T, Sawaguchi T, Konno T, Takai M, Ishihara K. Preparation of molecular dispersed polymer blend composed of polyethylene and poly(vinyl acetate) by in situ polymerization of vinyl acetate using supercritical carbon dioxide. Polymer 2007;48(6):1573–80.

Biomaterials 31 (2010) 4009–4016

Contents lists available at ScienceDirect

Biomaterials

journal homepage: www.elsevier.com/locate/biomaterials

The prevention of peritendinous adhesions by a phospholipid polymer hydrogel formed in situ by spontaneous intermolecular interactions

Noriyuki Ishiyama [a], Toru Moro [b], Kazuhiko Ishihara [c,d,e,*], Takashi Ohe [a], Toshiki Miura [a], Tomohiro Konno [d,e], Tadashi Ohyama [f], Mizuna Kimura [f], Masayuki Kyomoto [b], Kozo Nakamura [a], Hiroshi Kawaguchi [a]

[a] Sensory & Motor System Medicine, The University of Tokyo, 7-3-1 Hongo, Bunkyo-ku, Tokyo 113-8655, Japan
[b] Science for Joint Reconstruction, The University of Tokyo, 7-3-1 Hongo, Bunkyo-ku, Tokyo 113-8655, Japan
[c] Department of Materials Engineering, The University of Tokyo, 7-3-1 Hongo, Bunkyo-ku, Tokyo 113-8656, Japan
[d] Department of Bioengineering, The University of Tokyo, 7-3-1 Hongo, Bunkyo-ku, Tokyo 113-8656, Japan
[e] Center for NanoBio Integration, The University of Tokyo, 7-3-1 Hongo, Bunkyo-ku, Tokyo 113-8656, Japan
[f] Central Research Laboratories, Kaken Pharmaceutical Corporation, Yamashina, Kyoto 607-8042, Japan

ARTICLE INFO

Article history:
Received 18 December 2009
Accepted 15 January 2010
Available online 10 February 2010

Keywords:
Anti-adhesion
Tendon
Phospholipid polymer
Hydrogel
Biocompatibility

ABSTRACT

Preventing peritendinous adhesions after surgical repair of tendon is difficult. In order to establish an ideal anti-adhesion material, we prepared a spontaneously forming hydrogel by mixing the aqueous solutions of two polymers, poly(MPC-*co*-methacrylic acid) (PMA) and amphiphilic poly(MPC-*co*-*n*-butyl methacrylate) (PMB), in the presence of Fe^{3+}. This PMA/PMB/Fe^{3+} hydrogel (MPC polymer hydrogel) had a honeycomb microstructure with nanometer-scale pores, which resist cell invasion but allow the passage of cytokines and growth factors for tendon healing. The dissociation rate of the hydrogel could be controlled by changing Fe^{3+} concentration, and by examining the viscoelasticity of the hydrogel, we determined the optimal Fe^{3+} concentration to be 0.05 M. We then examined the effects of the in situ application of this MPC polymer hydrogel containing 0.05 M Fe^{3+} by using two animal models: the rat Achilles tendon model and the chicken flexor digitorum profundus tendon model. In both models, macroscopic and histological observation revealed that peritendinous adhesions were significantly decreased by the hydrogel application. Mechanical analyses revealed that the hydrogel prevented peritendinous adhesions but did not affect the tendon healing. Because of its characteristic microstructure and excellent biocompatibility, we believe that the MPC polymer hydrogel will be ideal for preventing peritendinous adhesions.

1. Introduction

The successful repair of sutured tendons, especially digital flexor tendons in zone II, is a major challenge for hand surgeons. The most common complication after tendon repair is the loss of digital motion as a result of restrictive adhesions between the tendon and the surrounding tissues [1,2]. Tendon healing proceeds by a combination of extrinsic and intrinsic processes. Previously, it was thought that peritendinous adhesions contributed to the healing process, since the chemotaxis of precursor cells into the defect was believed to be an essential extrinsic process of tendon healing [3,4]. Now, however, it is well known that tendon healing can, and ideally should, occur in the absence of peritendinous adhesions and through the intrinsic process: by the activity of tenocytes in the tendon sheath with sufficient supplies of cytokines and growth factors from the outside [5,6]. Despite advances in surgical techniques and rehabilitation programs [7,8], the results of tendon repair within the sheath remain largely unpredictable [1,2]. Hence, many modalities have been investigated to prevent adhesion formation such as the use of pharmacologic modulators or mechanical barriers between the tendon and surrounding tissues [9–18].

Hydrogels have recently received attention because they are useful and handy biomaterials in various medical fields. In order to find materials that can prevent peritendinous adhesions while allowing tendon healing, we focused on hydrogels that can resist cell adhesion and are highly permeable to nutrients. We have

* Corresponding author at. Department of Materials Engineering, The University of Tokyo, 7-3-1 Hongo, Bunkyo-ku, Tokyo 113-8656, Japan. Tel.: +81 3 5841 7124; fax: +81 3 5841 8647.
E-mail address: ishihara@mpc.t.u-tokyo.ac.jp (K. Ishihara).

0142-9612/$ – see front matter © 2010 Elsevier Ltd. All rights reserved.
doi:10.1016/j.biomaterials.2010.01.100

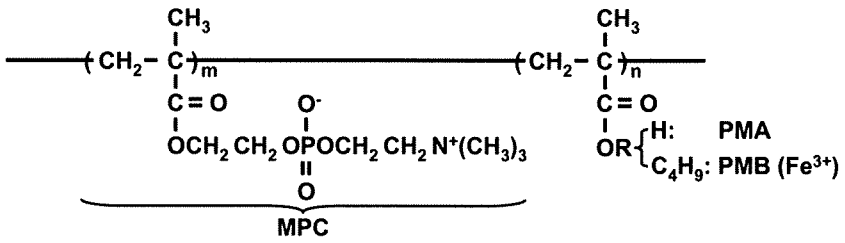

Fig. 1. Chemical structure of the two MPC polymers (PMA and PMB). Both polymers became aqueous solutions when they contained the hydrophilic MPC polymer.

reported that the 2-methacryloyloxyethyl phosphorylcholine (MPC) polymers have excellent antithrombogenicity and cytocompatibility and do not react to endogenous proteins and cells [19,20]. These properties are based on effective suppression of protein adsorption at the MPC polymer surface. We have therefore prepared a hydrogel by mixing aqueous solutions of two MPC polymers, poly[MPC-*co*-methacrylic acid(MA)] (PMA) and poly[MPC-*co*-*n*-butyl methacrylate(BMA)] (PMB), at room temperature without any chemical treatment [21,22]. The PMA/PMB hydrogel is formed by molecular interactions such as hydrogen bonding and hydrophobic interactions, and it is expected to be promising for in situ setting because of its excellent biocompatibility and dissociation ability. This hydrogel also prevents cell invasion but is highly permeable to cytokines and growth factors [23,24]. However, since the PMA/PMB hydrogel has a short dissociation time under physiological conditions, it cannot remain at the sutured site during the critical period up to 3 weeks. To overcome this problem, we introduced another mechanism, ionic crosslinking, for crosslinking the counter cations and carboxylate anions in the PMA/PMB hydrogel in order to achieve stabilization. Although Na^+ and Ca^{2+} did not show the expected stabilization effect, the stability of the PMA/PMB hydrogel containing Fe^{3+} (MPC polymer hydrogel) improved in a large amount of the aqueous medium [21]. Hence, we first sought to determine the optimal concentration of Fe^{3+} required for use of the MPC polymer hydrogel for adhesion resistance. Then, we examined the effects of the in situ application of this hydrogel on peritendinous adhesions and tendon healing by using two independent animal models.

2. Materials and methods

2.1. Preparation of hydrogel composed of PMA and PMB

MPC was synthesized according to the method reported previously [25]. PMA (number-average molecular weight [Mn] = 2.7×10^5, weight-average molecular weight [Mw] = 8.4×10^5, and MPC unit mole fraction in the polymer = 0.30) and PMB (Mn = 1.1×10^5, Mw = 8.6×10^5, and MPC unit mole fraction in the polymer = 0.80) were synthesized by conventional radical polymerization of corresponding monomers and purified by a membrane filtration technique (Fig. 1). An equal amount (1.0 mL) of aqueous solutions of PMA and PMB (5.0 wt%) was added to a conical tube. The tube was sealed with a cap and shaken vigorously by hand at room temperature for 10 s. After 10–20 s, the mixture of these MPC polymer solutions was spontaneously transformed into a hydrogel state. A hydrogel containing Fe^{3+} (MPC polymer hydrogel) was prepared using PMB containing $FeCl_3$ (Kanto Chemical Co. Inc., Tokyo, Japan).

2.2. Stability of the MPC polymer hydrogel in vitro and in vivo

To evaluate the dissociation of the MPC polymer hydrogel in vitro, diffusion chambers (Millipore, Billerica, MA) containing the MPC polymer hydrogel (300 μL; Fe^{3+} concentration: 0, 0.005 M, 0.05 M, or 0.5 M) were immersed in phosphate-buffered saline (PBS; 30 mL). The chamber was weighed at specific time intervals to determine the weight of the remaining hydrogel.

All animal experiments were performed according to the protocol approved by the Animal Care and Use Committee of the University of Tokyo. To evaluate the in vivo stability of the MPC polymer hydrogel, a diffusion chamber containing the MPC polymer hydrogel above was subcutaneously implanted into the back of an 8-week-old Slc:Wistar rat (Sankyo Labo Service Co. Inc., Tokyo) under general anesthesia with tribromoethanol (400 mg/kg body weight; intraperitoneally [i.p.]; Sigma–Aldrich Co., St. Louis, MO). After 7 or 21 days, the chamber was removed, and the viscoelastic properties of the hydrogel were investigated with a rheometer (Rheolograph-Micro, Toyoseiki, Tokyo). The extracted hydrogel was slowly inserted into both sides of a vibration blade. Immediately after the insertion, the blade was set in motion (vibrational amplitude: 200 μm; frequency: 20 Hz) and the elastic modulus and viscous modulus were recorded [26]. The elastic modulus is related to the energy stored in the sample to resist deformation and is a measure of the strength of the gel. The viscous modulus is a measure of the energy dissipated when the sample is deformed. The conditions under which the elastic modulus becomes larger than the viscous modulus indicate the properties of the gel [27]. To evaluate the actual changes in the microstructure during the dissociation process, we observed the hydrogel with a scanning electron microscope (SM-200; Topcon Co., Tokyo).

2.3. Rat Achilles tendon model

Under general anesthesia with pentobarbiturate (50 g/kg body weight; i.p.; Dainippon Sumitomo Pharma Co., Ltd., Osaka, Japan), the right hind limbs of seven-week-old Slc:Wistar rats (Sankyo Labo Service Co. Inc., Tokyo) were shaved and prepared for aseptic surgery. The Achilles tendon was approached by a posterior skin incision and freed from the surrounding tissue. After cutting the tendon with a scalpel at 5 mm above its insertion to the calcaneus, it was sutured using a Kessler stitch with 6–0 braided polyester (Ethibond; Johnson & Johnson, New Brunswick, NJ) [28]. The animals were then randomly divided into two groups and either MPC polymer hydrogel (MPC group in the figure) or distilled water (control group in the figure) was injected around the repaired tendon (n = 6/group). After skin closure, the leg was immobilized in a cast to control the movement of the talocrural joint. The rats were allowed unrestricted activity and received food and water *ad libitum*. For macroscopic and biomechanical analyses, the rats were sacrificed 21 days after the surgery.

2.4. Chicken flexor digitorum profundus (FDP) tendon model

The chicken FDP tendon model was chosen because the length of the tendon would facilitate biomechanical analysis; further, the flexor mechanism in the chicken has been shown to be analogous to that of the human digit [29]. Under general anesthesia with intramuscular injections of ketamine (20 mg/kg body

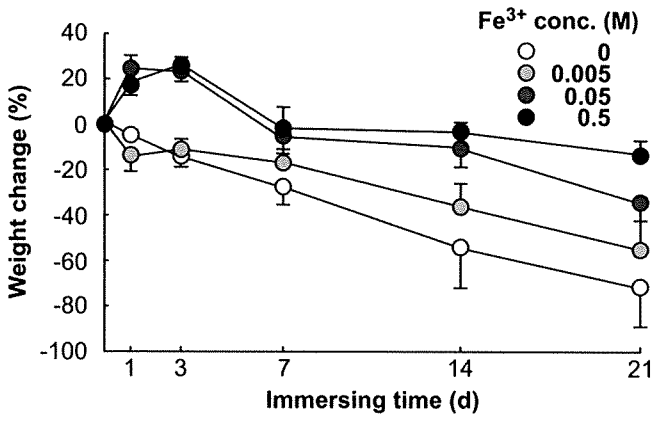

Fig. 2. Time course of dissociation of the MPC polymer hydrogel containing several concentrations (0–0.5 M) of Fe^{3+} determined by the weight change in a diffusion chamber that was immersed and gently stirred in PBS. Data are expressed as means (symbols) ± S.E. (error bars) for 6 hydrogels/group.

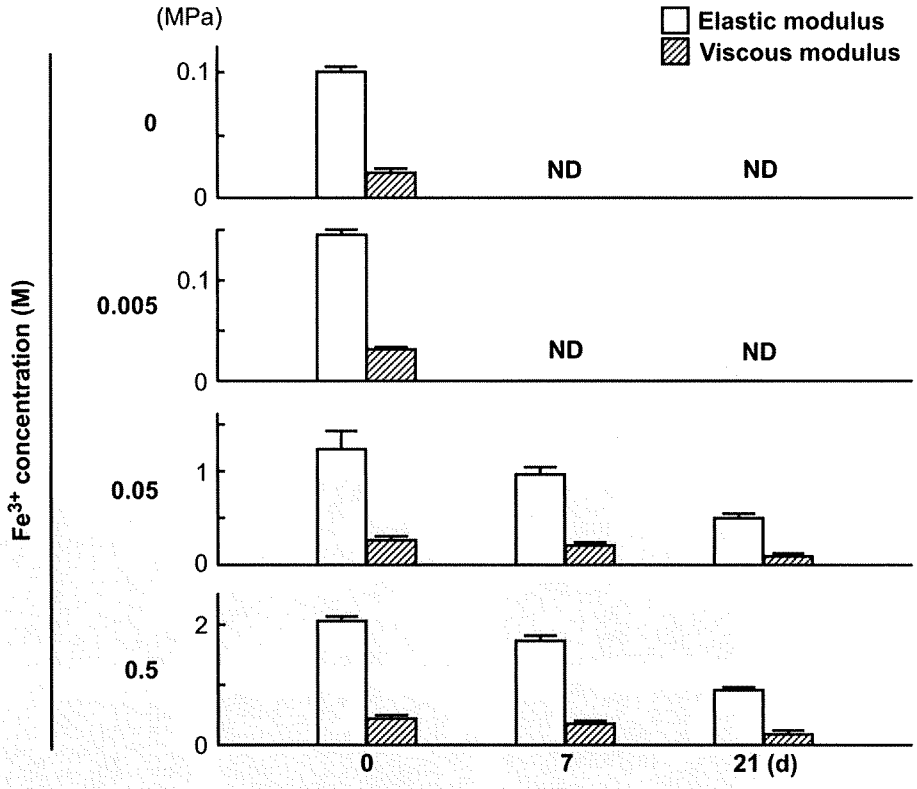

Fig. 3. Viscoelasticity of the MPC polymer hydrogel containing several concentrations (0–0.5 M) of Fe^{3+} before (0) and after (7 and 21 days) subcutaneous implantation in rats. The elastic and viscous moduli were measured using a rheometer. Higher elastic modulus than viscous modulus indicates gel properties. Data are expressed as means (bars) ± S.E. (error bars) for 3 hydrogels/group. ND; not detectable.

weight; intramuscularly [i.m.]; Daiichi Sankyo Propharma Co. Ltd., Tokyo) and xylazine (4 mg/kg body weight; i.m.; Bayer, Leverkusen, Germany), the FDP tendon of 5-month-old white Leghorn chicken (Shimizu Laboratory Supplies, Kyoto, Japan) was exposed through a midlateral incision in zone II, in which adhesion formation was caused by poor differential gliding between the superficial and the profundus tendons. The FDP tendon was delivered through the tendon sheath, divided, and then cut with a scalpel just distal to the chiasm and proximal to the vincula. Ruptured tendons were repaired using a Kessler stitch with 6–0 braided polyester [30]. The animals were then randomly divided into two groups and either MPC polymer hydrogel (MPC in the figure) or distilled water (control in the figure) was injected around the repaired tendon ($n = 16$ for MPC group and $n = 15$ for control group). After skin closure, the operated leg was padded and immobilized in a cast. The animals were allowed unrestricted activity and received food and water *ad libitum*. For macroscopic, histological and biomechanical analyses, the animals were sacrificed 21 days after the surgery.

2.5. Macroscopic evaluation

Before sacrificing the animals, the skin incision site was visually examined to check for any sign of inflammation and to confirm wound healing. To evaluate peritendinous adhesions, we counted the number of fibrous adhesions around the sutured tendon which required sharp dissection for release. In addition, to analyze the extent of adhesion formation, we evenly divided the tendon surface into 40 areas and used two evaluation parameters, the adhesion score and adhesion rate, for this purpose. The adhesion score was used to categorize the severity of adhesion at a particular area into grade 1–5 on the basis of the surgical findings: grade 1, no adhesion; grade 2, adhesion can be separated by blunt dissection alone; grade 3, sharp dissection is required to separate less than or equal to 50% of the adhesion area; grade 4, sharp dissection is required to separate 51–97.5% of the adhesion area; and grade 5, sharp dissection is required to separate more than 97.5% of the adhesion area [31]. The adhesion rate was used to quantify the severity of adhesion of the tendon as a whole. We counted the number of areas that needed sharp dissection to separate the adhesion and multiplied this number by 2.5%. For example, when 8 of the 40 areas were classified as grades 3 to 5, we calculated the extent of scar formation as 20%. These three parameters were evaluated by a single observer who was blind to the experimental group.

2.6. Histological evaluation

The third toe of the chickens was dissected and fixed for 1 week at room temperature in 4% paraformaldehyde buffered with PBS (pH 7.4). The specimens were decalcified for 1 week with 10% formic acid at room temperature. After dehydration with an increasing concentration of ethanol and embedment in paraffin, 4-μm-thick sagittal sections were obtained. To evaluate peritendinous adhesions and tendon healing, the sections were stained with Azan (Muto Pure Chemicals Co. Ltd., Tokyo), according to standard procedures. These histological sections were evaluated microscopically (AX-80; Olympus, Tokyo) by a single observer (double-blinded) for the presence of fibrous adhesion around the tendon and the extent of normal tendon healing at the sutured site.

2.7. Biomechanical evaluation

To evaluate peritendinous adhesions and tendon healing, the work of flexion and maximal tensile strength, respectively, were measured using a rheometer (CR-500-DX-LII; Sun Scientific, Tokyo). The work of flexion represents the work necessary to overcome the resisting forces from within the tendon sheath. After 21 days of surgery, the chicken third toes of both limbs were harvested with the flexor tendon and sheath intact. The proximal end of the FDP tendon was attached to the crosshead nonslip clamp of the rheometer. The actuator pulled the tendon at 20 mm/min, till 135° flexion. The force and the excursion of the clamp were measured directly, and the work of flexion was calculated by curve integration. The adhesion-related work of flexion in each animal was the ratio of the work of flexion in the injured and the uninjured digit [32]. The maximal tensile strength represented the breaking strength at the repair site. After 21 days of surgery, the repaired rat Achilles tendons and chicken FDP tendons were harvested for evaluation of the tensile strength. The proximal and distal ends of the tendon were fixed with nonslip clamps attached to the rheometer. The actuator pulled the tendon at 20 mm/min, till terminal rupture was achieved. In this case, the rheometer recorded the maximal tensile force [33].

2.8. Statistical analysis

The data were analyzed by the Mann–Whitney *U* test, and *P*-values less than 0.05 were considered significant.

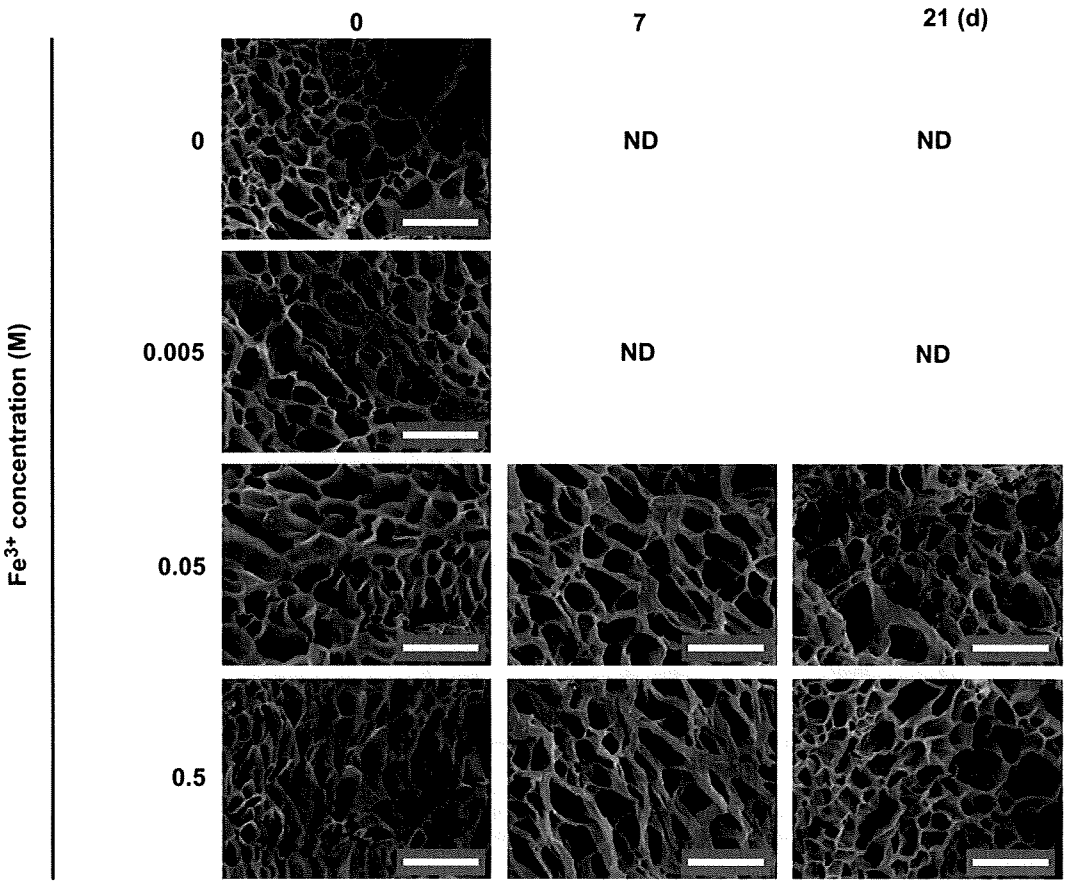

Fig. 4. Scanning electron microscopy images of the MPC polymer hydrogel containing several concentrations (0–0.5 M) of Fe^{3+} before (0) and after (7 and 21 days) subcutaneous implantation in rats. Scale bars, 30 μm. ND; not detectable.

3. Results

3.1. Determination of Fe^{3+} concentration in the MPC polymer hydrogel

Since the Fe^{3+} concentration in PMB is known to control crosslinking between PMA and PMB [26], we initially sought to determine the concentration required to prepare MPC polymer hydrogel with optimal viscoelasticity. The hydrogel was successfully formed immediately after mixing PMA and PMB, regardless of the Fe^{3+} concentration (0–0.5 M) in PMB. To compare the in vitro stability of the MPC polymer hydrogel formed from several concentrations of Fe^{3+}, we examined the time course of weight change of the hydrogel in a diffusion chamber which was immersed and gently stirred in PBS (Fig. 2). The dissociation was prevented dependently on the Fe^{3+} concentrations, confirming that Fe^{3+} increased the density of crosslinking and the stability of hydrogel, as reported previously [26].

We then examined the effects of Fe^{3+} concentration on the in vivo stability of the MPC polymer hydrogel for 21 days after the subcutaneous implantation in rats (Figs. 3 and 4). Measurements of elastic and viscous moduli revealed that MPC polymer hydrogel containing 0.05 M or 0.5 M Fe^{3+} similarly kept the gel properties shown by higher levels of elastic modulus than viscous modulus for at least 21 days after the implantation (Fig. 3). Scanning electron microscopic analyses showed that MPC polymer hydrogel

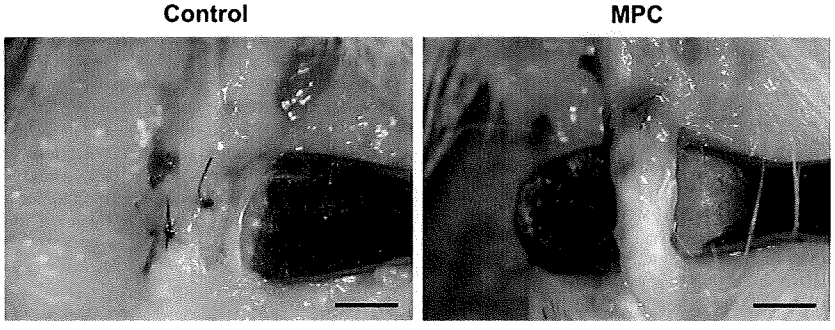

Fig. 5. Peritendinous adhesions shown by passage of a spatula under the sutured tendon 21 days after the local application of distilled water (control) or the MPC polymer hydrogel containing 0.05 M Fe^{3+} in the rat Achilles tendon model. Scale bars, 2 mm.